



Norwegian University of
Science and Technology

Advanced analysis of measured data for efficient operation of modern buildings

Francois Leboeuf

Master of Science in Energy and Environment

Submission date: June 2011

Supervisor: Vojislav Novakovic, EPT

Norwegian University of Science and Technology
Department of Energy and Process Engineering



**Advanced analysis of measured data for efficient operation
of modern buildings**

Abstract

The aim of this study is to define several methods that enable to estimate the heat exchanged in the different components of an air handling unit (AHU), and propose control strategy optimizations. The AHU studied is a part of a low energy office building located in Norway. The focus is especially made on its rotary heat recovery system, its heating/cooling coil and its heating coil. The data of one month recorded by the building energy management system (BEMS) have been used. The heat exchanged estimation methods presented in this paper are based on heat balances, valve positions and heat exchangers number of transfer unit (NTU). Comparison of the results obtained with the different methods outlined a poor quality of the valves positions signals. This fact has also been confirmed using a statistical method, the principal component analysis (PCA). Because of this issue, the methods proposed have not been validated. Regarding control strategy optimization, the use of a heat exchanged estimation method is required. The estimation method based on NTU has been used as reference, since this method does not use the valves positions signals. The goals of control strategy optimization are to reduce the energy costs and the CO₂ emission. The proposed improvements are based on a new distribution between components of input heat, regarding the specific energy cost and CO₂ emission of components. The tested optimizations gave better results than the current control strategy, but since the method used as reference has not been validated, these conclusions have to be confirmed after a resolution of the valves positions signals problems.

French Abstract

Le but de ce projet est de définir des méthodes permettant d'estimer la chaleur échangée dans les différents systèmes thermiques d'une centrale de traitement d'air (CTA), et de proposer des optimisations de la stratégie de contrôle de ces éléments. La CTA étudiée se trouve dans un immeuble de bureaux, à faible consommation d'énergie, situé à Trondheim, en Norvège. Cette mission est étroitement liée au projet de recherche "lifetime commissioning" au sein de NTNU (Norges teknisk-naturvitenskapelige universitet) et SINTEF (PKF). Ce projet de recherche national a pour objectif le développement d'outils et de méthodes pour l'amélioration des procédures de suivis et des contrôles qualités des performances des bâtiments.

Le bâtiment qui fait l'objet de notre étude a une surface chauffée de 16 200 m², répartis sur six étages. Il est en service depuis le mois de septembre 2009. La température extérieure de dimensionnement est -19°C et la température moyenne annuelle est 6°C. Le bâtiment comporte des systèmes de chauffage, de climatisation et de ventilation. Le chauffage est assuré par des radiateurs et la climatisation par des ventilo-convecteurs. En ce qui concerne la ventilation, elle consiste en huit CTA à volume d'air variable (débit maximal de 12 500 m³/h à 22 000m³/h). La puissance chaude pour la ventilation, le chauffage et l'eau chaude sanitaire est fournis par le réseau de chaleur urbain et des pompes à chaleurs. La puissance de refroidissement est fournie par deux groupes froids. La chaleur dégagée par les condenseurs de ces groupes froids est utilisé comme énergie additionnelle pour le chauffage. En ce sens, ces groupes froids peuvent être considérés comme des pompes à chaleurs. L'un des groupes froids est utilisé pour les ventilo-convecteurs, et l'autre est uniquement utilisé pour la ventilation. Le projet de recherche [6] qui a précédé ce master recherche s'est principalement focalisé sur ce dernier groupe froid, et particulièrement sur la détection d'erreurs au niveau de ces capteurs de mesures. Ici il est également question de ce groupe froid/pompe à chaleur, mais l'intérêt est principalement porté sur l'une des huit CTA.

La CTA concerné, présenté en *Figure 3*, à un débit d'air maximale de 15 000 m³/h. Elle comporte un système de récupération de chaleur rotatif qui permet un échange de chaleur entre arrivée et retour d'air, sans mélange. Il s'agit en fait d'une roue composée de fines plaques d'aluminium brasées (matrice). Lorsque la roue tourne, les plaques sont chauffées par l'air chaud et ces dernières restituent cette chaleur à l'air froid.

La CTA possède également une batterie chaude/froide et une batterie chaude. La batterie chaude/froide est relié à la pompe à chaleur précédemment cité (étudié lors du projet de recherche [6]). Elle peut donc fournir du chaud ou du froid, en fonction du mode de la pompe à chaleur. Sa capacité nominale est de 63,28 kW [10]. La puissance qui y est échangé est contrôlé via une vanne trois voies montés en répartition (température d'arrivée constante, débit variable). La batterie chaude est quant à elle alimentée par le réseau de chaleur urbain. Sa capacité nominale est de 41,68 kW [10]. La puissance qui y est échangé est contrôlé via une vanne trois voies montés en mélange (débit d'arrivée constant, température variable).

Les différents systèmes thermiques et de ventilation du bâtiment sont contrôlés via un BEMS (Building Energy Management System). Ce dernier permet également d'enregistrer les valeurs des différents capteurs et signaux présent dans ces systèmes (les capteurs disponibles nous concernant sont présentés dans la "*List of symbols*" ainsi que dans les *Figure 2, Figure 3, Figure 8, Figure 9, Figure 10*. Ils font également bien entendu l'objet d'une sous-partie : "Available Data From The Monitoring System"). Le travail présenté ici se base sur les données relevées par le BEMS pour le mois de Mars 2011, avec pour base de temps la minute.

De manière générale, les systèmes de traitement d'air ont un rôle de plus en plus important au niveau de la qualité de l'air intérieur. En effet, dans un contexte de recherche constante de diminution de la consommation d'énergie, les bâtiments sont de mieux en mieux isolés (isolation thermique au niveau des murs, fenêtres à double ou triple vitrage, etc) et l'un des effets induits le plus important est la diminution des infiltrations d'air et donc de la ventilation naturelle. D'où le rôle de plus en plus important des systèmes de ventilation au niveau de la qualité de l'air intérieur, du confort thermique mais également en tant que source de consommation d'énergie.

Dans ce projet l'accent est porté sur la consommation d'énergie, mais aussi sur les aspects environnementaux. Dans un premier temps la contribution du système de récupération de chaleur et des deux batteries est déterminée. Il s'agit d'une première étape dans la proposition d'optimisations de la stratégie de contrôle de la CTA. Pour ce faire plusieurs méthodes sont utilisées : bilan de chaleur, pourcentage d'ouverture de vanne, Nombre d'unité de transfert (NUT). Ces méthodes sont en fait des mesures virtuelles. Elles sont basées sur les relevés du BEMS.

La méthode se basant sur les bilans de chaleur suit un principe assez simple : Dans un échangeur thermique, la chaleur perdue par un fluide est gagnée par l'autre fluide. Aussi si le débit et la différence de température pour un fluide est connue on peut déterminer la chaleur échangée. Par ailleurs si pour l'autre fluide, le débit et au moins une température (entrée ou sortie) est connue, on peut retrouver la température manquante. Plus généralement, sur six variables (*débit du fluide un, température d'entrée du fluide un, température de sortie du fluide un, débit du fluide deux, température d'entrée du fluide deux, température de sortie du fluide deux*), nous avons besoin de connaître cinq d'entre elles (*plus les paramètres physiques des deux fluides, tels que la chaleur spécifique C_p et éventuellement la masse volumique ρ*). En outre dans le cas des deux batteries, les signaux de positions des vannes trois sont utilisés pour déterminer la température (ou le débit) d'entrée en fonction des caractéristiques, paramètres et type de montage de ces vannes, bien que des hypothèses doivent être faites sur ces éléments en raison d'un manque d'informations.

La méthode se basant sur le pourcentage d'ouverture de vanne ne s'applique qu'aux batteries. Les caractéristiques des vannes sont supposées être à égale à pourcentage (voir "*Three Way Valves*" et "*Heating Coil, LV*"), aussi la relation entre pourcentage d'ouverture de vanne et puissance chaude fournie est linéaire comme le montre la *Figure 7*. Pour obtenir la

puissance échangée dans chaque batterie il suffit donc de multiplier le pourcentage d'ouverture de leur vanne par leur puissance nominale.

Enfin la méthode se basant sur le NUT est également uniquement dédiée aux batteries. Cette méthode utilise les caractéristiques intrinsèques aux échangeurs de chaleurs que sont les batteries : leur efficacité η , leur coefficient de transfert thermique h , leur surface d'échange S . h et S sont calculés ou donnés via la documentation du fabricant [10]. η et le NUT sont recalculés. Ils permettent de retrouver des températures manquantes. L'avantage de cette méthode est la non utilisation des positions des vannes (contrairement aux deux précédentes méthodes) et le nombre moins important de valeurs connues requises.

Une dernière méthode est utilisée dans cette étude. Il s'agit de l'analyse par composante principale ou "principal component analysis" (PCA). Contrairement aux méthodes présentées, cette dernière n'a pas pour but de déterminer la contribution de chaque composant dans la chaleur apportée à l'air. Cette méthode a été utilisée lors du projet de recherche [6] lié à ce master recherche, pour mettre en évidence des défauts au niveau des signaux des capteurs. PCA est une méthode statistique de modélisation bilinéaire qui utilise une transformation orthogonale. Elle permet de convertir les variables d'origines, qui sont supposés être corrélées, en un nouvel ensemble de variables non corrélées : les composantes principales. Le nombre de composante principale est inférieur ou égale aux nombre de variables d'origines. L'étude de ces composantes principales permet entre autre, via le tracé des résidus, de détecter des défauts au niveau des signaux des capteurs.

Les résultats comparatives des méthodes présentés (hors PCA) sont relativement différent, tend en terme de chaleur totale apportée au cours du mois étudié dans chaque composant, qu'au niveau de la chaleur apportée minute par minute. Une étude d'analyse de sensibilité des caractéristiques et paramètres des vannes est mené pour s'assurer que les hypothèses posées à ce sujet ne sont pas incriminées. Cette étude montre qu'en effet ces paramètres ont peu d'influence sur les résultats des différentes méthodes. La principale autre raison qui peut expliquer de telles différences dans les résultats est un défaut au niveau des signaux de position des vannes. En effet cette possibilité peut être envisagée au vu des différences de résultats en minute par minute entre les méthodes NUT et pourcentage d'ouverture de vanne, comme le montre la *Figure 13*. La méthode PCA est employée pour vérifier cette possibilité, et effectivement, les signaux de position des vannes présentes des irrégularités propres à une qualité très médiocre de l'information fournie.

L'un des principaux buts de cette étude est l'optimisation du la stratégie de contrôle de la CTA étudiée en vue d'une diminution du coût énergétique et/ou des émissions de CO_2 , induits par son utilisation. Pour ce faire une nouvelle distribution entre les différents composants (système de récupération de chaleur et les deux batteries) de la chaleur totale apportée doit être imaginée. Pour cela il est nécessaire de connaître la contribution actuelle de chaque équipement minute par minute. D'où le développement de différentes méthodes d'estimations, mentionnées précédemment.

Cependant en raison de défauts aux niveaux des signaux de position des vannes, il n'a pas été possible de valider les méthodes proposées. Néanmoins, la méthode NUT n'utilise pas les signaux incriminés. En conséquence les résultats obtenus avec cette méthode sont les plus à mêmes pour servir de référence. La stratégie actuelle de contrôle donne la priorité au récupérateur de chaleur, puis à la batterie chaude/froide et enfin à la batterie chaude. La comparaison des *Figure 25* (théorique) et *Figure 26* (pratique) semblent indiquer que cette stratégie n'est en fait pas complètement suivie. Cependant, en raison des défauts des signaux de position de vanne, il n'est pas possible de tirer de conclusion de cette comparaison.

Les coûts énergétiques et les émissions de CO₂ de chaque composant sont calculés en prenant en compte leurs performances et leurs sources d'énergie (COP de la pompe à chaleur, électricité fournie à partir de centrales hydrauliques (99%) et d'électricité européenne UCPTÉ (1%), et réseau de chaleur urbain alimenté par l'incinération de déchets). Ces estimations sont faites pour chaque minute.

Les nouvelles stratégies de contrôles proposées se basent sur le coût énergétique et les émissions de CO₂ totales, induite par la répartition entre les composants de la chaleur apportée à l'air, la quantité totale de chaleur devant être apportée restant constante. Deux stratégies sont donc définies. La première s'appuie sur une réduction du coût énergétique et la deuxième sur une réduction des émissions de CO₂. Le principe est simple, il s'agit de déterminer pour chaque minute, l'ordre des composants du plus économique au moins rentable (ou du plus environnementale au plus polluant). En terme de coût, le système de récupération de chaleur est toujours le plus économique. Puis vient la batterie chaude/froide si le prix unitaire de l'électricité divisé par le COP de la pompe à chaleur est inférieur au prix unitaire du réseau de chaleur urbain. Si ce n'est pas le cas c'est la batterie chaude qui sera la plus économique. Les puissances maximales fournissables par les batteries sont considérées égales à leur puissance nominale, renseignée par le fabricant [10]. En ce qui concerne le système de récupération de chaleur, la puissance maximale fournissable est en permanence recalculée en fonction de son efficacité maximale et des températures d'arrivée/retour d'air.

La comparaison des deux stratégies proposées à la stratégie actuelle est effectuée en deux temps. Tout d'abord l'impact entre la différence de prix unitaire de l'électricité et le réseau de chaleur urbain est étudié. Puis l'impact de l'origine de ces deux sources d'énergies sur les émissions de CO₂ est considéré.

Dans tous les cas de figures, les stratégies proposées donnent de meilleurs résultats que la stratégie actuelle, tant pour les coûts énergétiques que pour les émissions de CO₂. Cela est en grande partie dû à une sous-utilisation du système de récupération de chaleur dans la configuration actuelle.

Avec les paramètres propres à Trondheim (*électricité fournie à partir de centrales hydrauliques (99%) et d'électricité européenne UCPTÉ (1%), et réseau de chaleur urbain alimenté par l'incinération de déchets*) la batterie chaude/froide est avantageuse pour la stratégie basée sur une réduction des coûts, tandis que la batterie chaude est avantageuse pour la stratégie basée sur une réduction des émissions de CO₂. Cette dernière devient

également avantageuse pour la stratégie basée sur les coûts si le prix unitaire du réseau de chaleur urbain est fortement réduit et que le prix unitaire de l'électricité reste stable.

En ce qui concerne les émissions de CO₂, les deux stratégies donnent des résultats similaires si l'électricité provient de centrale hydrauliques (99%) et d'électricité européenne (1%), et que le réseau de chaleur urbain est alimenté par l'incinération de bois.

Dans cette étude les coûts énergétiques et les émissions de CO₂ sont traités en grande partie séparément, cependant dans la réalité ils doivent être combinés. Par ailleurs bien que les stratégies proposées semblent meilleurs que la stratégie actuelle, ces résultats doivent être maniés prudemment. En effet, en raison de la qualité des mesures, les méthodes d'estimation de la chaleur apportée par chaque équipement n'ont pas été validées. Aussi ces mesures doivent être améliorées avant de pouvoir retester ces nouvelles stratégies de contrôle et d'éventuellement les valider.

Table of contents

Abstract	2
French Abstract	3
Table of contents	8
List of symbols	10
List of Figures and Tables	13
Introduction	15
System Presentation	16
Heat Pump System	16
Compressor	17
Condenser	18
Evaporator.....	19
Heat Pump Performance.....	19
Air Handling Unit	20
Rotary Heat Recovery System	21
Heating/Cooling Coil.....	22
Heating Coil	22
Three Way Valves	23
Available Data From The Monitoring System	25
Heat Pump and District Heating.....	25
Air Handling Unit	25
Determination of the heat exchanged in each component	27
Pre-processing.....	27
Heat Balance Method.....	28
Heat Recovery System, LX01	28
Heating Coil, LV	29
Heating/Cooling Coil, LK.....	31
Valve Position Method	32
NTU Method.....	33
Combination of the NTU and valve position methods.....	35
Principal Component Analyses (PCA) method	35
Results Interpretations.....	36

Heat Balance/ Valve Position/ NTU methods Comparison	36
PCA Applied On The Air Handling Unit Sensors	39
Optimization of control strategy in AHU	42
Current control rules	42
Energy Costs and CO ₂ emission	43
Rotary heat recovery system	44
Heating/cooling coil	44
Heating coil.....	45
Improved Control Strategies	45
Current and proposed rules comparisons.....	47
Conclusion	50
Acknowledgments	51
Appendix.....	52
Primary energy factors and CO ₂ emission coefficients	52
References.....	53

List of symbols

Nomenclature				
Symbol	Sensor	Signification	value	units
\dot{V}_s		Theoretical compressor volume flow rate	0,0373	m ³ /s
\dot{W}_d		Compressor power (direct)	no constant	kW
\dot{W}_{id}		Compressor power (indirect)	no constant	kW
\dot{W}_{loss}		Condenser electromechanical power losses	1001,377	W
\dot{W}_{FL}		Compressor power (full load)	no constant	kW
η		Compressor efficiency	0,837	
p_{dis1}	35.01 RP60	Discharge pressure circuit 1	no constant	bar
p_{dis2}	35.01 RP61	Discharge pressure circuit 2	no constant	bar
p_{suc1}	35.01 RP62	Suction pressure circuit 1	no constant	bar
p_{suc2}	35.01 RP63	Suction pressure circuit 2	no constant	bar
$p1$		Pourcentage of the full load (circuit 1)	no constant	
$p2$		Pourcentage of the full load (circuit 1)	no constant	
$\dot{Q}_{c,d}$		Condenser load (direct)	no constant	
$\dot{Q}_{c,id}$		Condenser load (indirect)	no constant	
$\dot{Q}_{c,FL}$		Condenser load (full load)	no constant	
\dot{V}_w		Calibrated water glycol volume flow rate	88	m ³ /h
ρ_{wg}		Water glycol density	1028	kg/m ³
Cp_{wg}		Water glycol Specific heat capacity	3,837	kJ/kg.K
ρ_w		Water density	1000	kg/m ³
Cp_w		Water Specific heat capacity	4,180	kJ/kg.K
T_{win}	35.01 RT50	Condenser water glycol return temperature	no constant	°C
T_{wout}	35.01 RT40	Condense water glycol leaving temperature	no constant	°C
γ		isentropic exponent	1,3	
C		Clearance factor	0,001	
UA		Overall Heat transfert coefficient	19183,906	W/K
m		exponent for heat exchanger	0,8	
T_{out}	35.01 RT90	Outdoor temperature (just used in the case of heat pump COP calculations)	no constant	°C
COP_{th}		Theoretical coefficient of performance	no constant	
COP_d		Coefficient of performance (direct)	no constant	
COP_{id}		Coefficient of performance (indirect)	no constant	
$COP_{th,FL}$		Coefficient of performance (interpol/extrapol. Of manufacturer data)	no constant	
ρ_{air}		Air density	1,005	kg/m ³
Cp_{air}		Air Specific heat capacity	1,2	kJ/kg.K
\dot{V}_{sair_max}		Supply maximal air flow rate	15 000	m ³ /s
\dot{V}_{rair_max}		Return maximal air flow rate	15 000	m ³ /s
\dot{V}_{LK}		Heating/cooling coil water maximal flow rate	10,264	m ³ /h
\dot{V}_{LV}		Heating coil water flow rate	1,224	m ³ /h
$\dot{Q}_{LK\ max}$		Maximal heat exchanged in the heating/cooling coil	63,28	kW

		(manufacturer data)		
\dot{Q}_{LV_max}		Maximal heat exchanged in the heating coil (manufacturer data)	41,68	kW
T_{LV_dh}	32.01 RT40	District heating provided temperature	no constant	°C
A		Three way valves authority	0.5	
R		Three way valves range	40	
x_p		Three way valves - percentage of the maximal flow rate	no constant	
T_{out}	36.05 RT90	Outside temperature (not used in the case of heat pump COP calculations)	no constant	°C
T_{sair_hr}		Supply Air temperature after heat recovery system	no constant	°C
T_{sair_LK}		Supply Air temperature after the heating/cooling coil	no constant	°C
T_{sair}	36.05 RT40	Supply air temperature (T_{sair})	no constant	°C
T_{sair_des}	36.05 RT40SPK	Supply air desired temperature	no constant	°C
T_{rair}	36.05 RT50	Return Air temperature	no constant	°C
T_{rair_hr}	36.05 RT54	Return Air temperature after heat recovery system	no constant	°C
T_{LK_win}		Heating/cooling coil water inlet temperature	no constant	°C
T_{LK_wout}		Heating/cooling coil water outlet temperature	no constant	°C
T_{LV_win}		Heating coil LV inlet water temperature	no constant	°C
T_{LV_wout}	36.05 RT55	Heating coil LV outlet water temperature	no constant	°C
x_{JV40}	36.05 JV40	Supply fan signal, percentage of maximal supply air flow rate	0 to 100	%
x_{JV50}	36.05 JV50	Return fan signal, percentage of maximal return air flow rate	0 to 100	%
x_{LX01}	36.05 LX01	Heat recovery signal, percentage of maximal wheel speed	0 to 100	%
x_{LK}	36.05 LK40	Three way valve signal of the Heating/Cooling coil, percentage of valve opening (x_{LK})	0 to 100	%
x_{LV}	36.05 LV40	Three way valve signal of the Heating coil, percentage of valve opening (x_{LK})	0 to 100	%
p_{sup}	36.05 RP40	Supply air pressure	no constant	Pa
p_{ret}	36.05 RP50	Return air pressure	no constant	Pa
\dot{W}_{hr_max}		Maximal power of the heat recovery motor	100	W
η_{hr}		Heat recovery efficiency	no constant	
η_{hr_max}		Heat recovery maximal efficiency	Calcul. 0,85	
\dot{Q}_{hr}		Heat exchanged in the heat recovery	no constant	kW
$\dot{Q}_{LK_hb_air}$		Heat exchanged in the heating/cooling coil calculated with heat balance method (based on air temp.)	no constant	kW
$\dot{Q}_{LK_hb_wat}$		Heat exchanged in the heating/cooling coil calculated with heat balance method (based on water temp.)	no constant	kW
\dot{Q}_{LV_hb}		Heat exchanged in the heating coil calculated with heat balance method	no constant	kW
\dot{Q}_{LK_x}		Heat exchanged in the heating/cooling coil calculated with valve position method	no constant	kW
\dot{Q}_{LV_x}		Heat exchanged in the heating coil calculated with valve position method	no constant	kW
\dot{Q}_{LK_NTU}		Heat exchanged in the heating/cooling coil calculated with NTU method on the heating coil	no constant	kW

\dot{Q}_{LV_NTU}		Heat exchanged in the heating coil calculated with NTU method	no constant	kW
el_price		Electricity price		NOK/kWh
dh_price		District heating price		NOK/kWh
el_CO ₂		Electricity CO ₂ emission		kg/kWh
dh_CO ₂		District heating CO ₂ emission		kg/kWh
$Cost_{LK}$		Cost induced by heat exchanged in the heating/cooling coil	no constant	NOK
$Cost_{LK}$		Cost induced by heat exchanged in the heating coil	no constant	NOK
CO_{2_LK}		CO ₂ emission induced by heat exchanged in the heating/cooling coil	no constant	kg or ton
CO_{2_LV}		CO ₂ emission induced by heat exchanged in the heating coil	no constant	kg or ton

List of Figures and Tables

Figure 1. Office building in Trondheim.....	16
Figure 2. Schematic of heat pump	17
Figure 3. Schematic of Variable Air Volume Studied	21
Figure 4. Heating/cooling coil	22
Figure 5. Heating coil.....	23
Figure 6. Control Valve Flow Characteristics.....	24
Figure 7. Heat Output, Flow, and Stem Travel Characteristics of Equal Percentage Valve.....	25
Figure 8. Rotary heat recovery system – heat balance.....	29
Figure 9. Heating coil – heat balance/valve equation.....	30
Figure 10. Heating/Cooling coil – heat balance/valve equation.....	31
Figure 11. Total heat exchanged in each component during March 2011 determined with proposed methods	36
Figure 12. Total heat exchanged in the two coils during March 2011 determined with heat balance, valve position and NTU methods	37
Figure 13. Heat exchanged in the heating coil: NTU /valve position methods (minute basis)	38
Figure 14. Heat exchanged in the heating/cooling coil heat balance (based on air temperature)/valve position methods (minute basis).....	38
Figure 15. LX01 – x_{LX01} , Q-residuals (PC3)	40
Figure 16. LK40 - x_{LK} , Q-residuals (PC3).....	40
Figure 17. LV40 - x_{LV} , Q-residuals (PC3).....	40
Figure 18. JV40 – x_{JV40} , Q-residuals (PC3).....	40
Figure 19. JV50 – x_{JV50} , Q-residuals (PC3).....	40
Figure 20. RT90 - T_{out} , Q-residuals (PC3)	40
Figure 21. RT50 - T_{rair} , Q-residuals (PC3)	41
Figure 22. RT54 – T_{rair_hr} , Q-residuals (PC3).....	41
Figure 23. RT40 - T_{sair} , Q-residuals (PC3)	41
Figure 24. RT55 – T_{LV_wout} , Q-residuals (PC3).....	41
Figure 25. Winter control rules	43
Figure 26. Control rules verification.....	43
Figure 27. Heat pump COP (march 2011)	45
Figure 28. Improved control rules proposition: Cost strategy.....	46
Figure 29. Improved control rules proposition: CO ₂ strategy.....	46
Figure 30. efficiency of the heat recovery in function of its measured signal.....	47
Figure 31. Impact of the ratio district heating/electricity price on the costs	48
Figure 32. CO ₂ emission regarding sources of electricity and district heating	49
Table 1. Heat pump performance data in cooling mode	18
Table 2. Heat pump performance data in heating mode	18
Table 3. Compressor partial load	18

Table 4. Valves characteristics and parameters influence on Heat balance and valve position methods 39

Introduction

According to the European Environment Agency, energy consumption increased from 1125 million tons of oil equivalent (TOE) in 1995 to 1252.5 TOE in 2005, in the European Economic Area. In Norway it increased from 16.1 to 18.6 TOE and in France from 135.4 to 158.2 TOE. In the same time, the proportion of energy used for residential and tertiary sectors stayed quite constant in Europe. Indeed with around 40%, this is the most energy consumer sector. By the way, considering the diminution of classical sources of energy that provokes a quick rise of energy costs and bad effects that that kind of energy have on environment, it becomes more and more important to reduce our energy consumption, especially in buildings sector [1].

There are many domains that should be considered in the life of a building in order to achieve that purposes. The first one is the building design: shape, good orientation, materials used, insulation, efficient ventilation, and good selection and good design of heating systems. Then procedures of maintenance (preventive and curative) and quality control have to be put in place for the whole lifetime of the building. Regarding preventive maintenance and quality control, appears the requirement on knowledge of data and measurements, and correlations between them and standards. This point has to be considered in every phases of building life, and it starts in its conception. As explained in the work of Djuric and Novakovic [2], the Norwegian lifetime commissioning (LTC) procedures permit to do it. Moreover this is a recognized tool to perform a follow-up of the building performance during its lifetime. Besides, in order to satisfy the increasing demands on indoor environment quality and decrease energy consumption, buildings electrical and mechanical equipments such as Heating Ventilation and Air Conditioning system (HVAC) become more and more complex. Consequently, another important point is the establishment of a building energy management system (BEMS) that can control and monitor these complex systems.

One of the most important procedures are the detection of sensors faults and components dysfunctions. Indeed, sensor faults may provoke a wrong monitoring and a not adapted control of system from the BEMS. Components problems may cause malfunction of the system and the deterioration of healthy components. Sensors and components faults diagnosis have been in particular treated by Wang and Xiao [3], Zhou et al. [4], Wang et al. [5]. The last important consideration is the optimization of BEMS control strategy. If control strategies are poor, it may seriously decrease the building overall energy efficiency

In this thesis focus was made on a low energy, office building located in Trondheim, Norway. Especially on one of its Air Handling Unit (AHU) and one of its heat pumps. Detection of heat pump sensors faults have been the main subject of the project thesis linked to this work [6]. Henceforth, several methods will be used to determine the contribution of each component and eventually highlight sensors problems. Then new control strategies for AHU will be proposed and tested. In a first part, the studied system will be presented. Then a focus will be made on methods used, the gotten results interpreted, and finally new control strategies will be presented.

System Presentation

The system studied is a part of a low energy, office building located in Trondheim, Norway, shown in *Figure 1*, where design outdoor temperature is -19°C , while the average annual outdoor temperature is 6°C . This building has six floors, a heated area of $16\,200\text{ m}^2$ and it has been in use since September 2009.



Figure 1. Office building in Trondheim

The building is provided with heating, cooling and ventilation systems. Heating is provided by radiators, while cooling is provided by fan-coils. Regarding the ventilation system, it consists of eight AHU, that are Variable Air Volumes (VAV) systems with a maximal air flow from $12\,500\text{ m}^3/\text{h}$ to $22\,000\text{ m}^3/\text{h}$.

Heating energy for ventilation, space heating, and domestic water is supplied by district heating and heat pumps. Cooling energy is supplied by two cooling plants. Heat realized from the cooling plant condensers is used as additional energy for heating. In that way these cooling devices can be considered in the same time as heat pumps. One of the cooling plants is used for fan coils, while the other one is only used for the ventilation systems. In this paper we are going to focus on this last cooling plant/heat pump and one of the eight AHU.

Heat Pump System

A heat pump is a thermal machine that is enabled to move heat from one location (at a lower temperature) to another (at a higher temperature). Thanks to a reversible valve, a heat pump can be used to provide heating or cooling. In other world a heat pump can change which exchanger is the condenser and which is the evaporator. The schematic of the studied heat pump is shown in *Figure 2*.

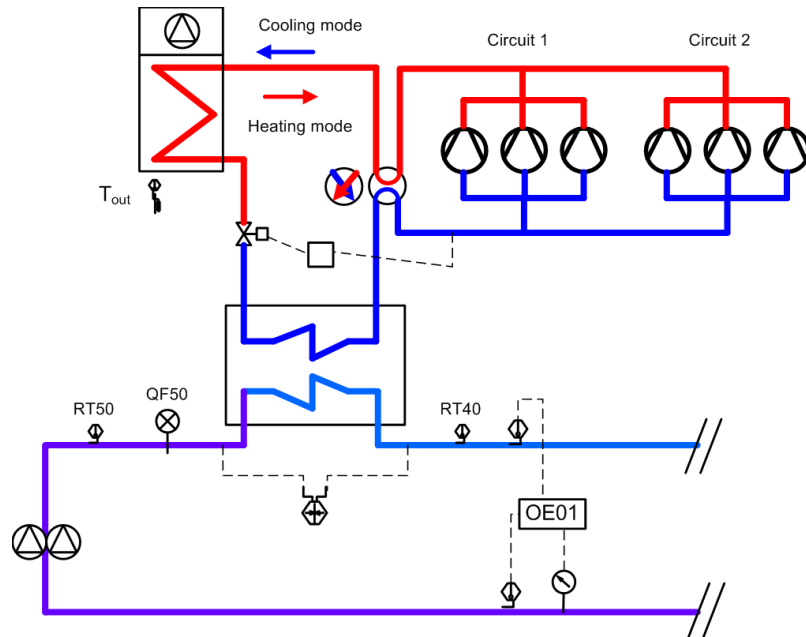


Figure 2. Schematic of heat pump

The heat pump used here is a model AQTH 1656. The refrigerant used is R410 A. The refrigerant circuit integrates a 4 ways reversing valve that allows the both modes utilization of this system (cooling and heating unit). Detailed technical information about the studied heat pump are given in the manufacturer data [7]. Each component of the heat pump in *Figure 2* and calculation of performance are explained in the further text.

Compressor

There are six hermetic scroll compressors arranged in trio configuration. The theoretical compressor volume flow rate (\dot{V}_s), is assumed to be constant and equal to $0.0373\text{m}^3/\text{s}$ (obtained by calibrating the model to the manufacturer data, as explained in [8]). The input power (for all compressors system) in full load depends on the condenser air temperature, the leaving water temperature and the used mode (heating or cooling unit). The compressor power in different modes is given in *Table 1* and *Table 2*. The use of six compressors in the same time or just some of them, enable to reduce the total cooling/heating capacity and also the total input power. Use of data in *Table 1* and *Table 2* and BEMS data enabled calculation of compressor input power. Indeed partial compressor load are monitored by the BEMS for the both group of 3 compressors (one step for each group). Each step (t) corresponds to a percentage of the full load, as presented in *Table 3*.

Table 1. Heat pump performance data in cooling mode

Cooling Capacities - AQTH STD/HSE/SIF - BLN Version

AQTH STD/HSE/SIF models	LWT (°C)	Condenser entering air temperature (°C)													
		25		30		32		35		40		44		46	
		Cool. cap. (kW)	Input power (kW)	Cool. cap. (kW)	Input power (kW)	Cool. cap. (kW)	Input power (kW)	Cool. cap. (kW)	Input power (kW)	Cool. cap. (kW)	Input power (kW)	Cool. cap. (kW)	Input power (kW)	Cool. cap. (kW)	Input power (kW)
1656 BLN	5	415.0	111.4	395.0	122.3	386.6	126.8	373.7	133.6	347.4	148.4	331.2	157.8	315.0	167.3
	6	427.4	112.7	406.5	123.7	398.1	128.2	384.7	135.1	357.8	149.9	341.0	159.5	324.3	169.0
	7	439.8	114.1	418.4	125.1	409.5	129.7	396.0	136.5	368.0	151.5	350.9	161.1	333.7	170.6
	8	450.8	115.4	429.0	126.5	420.0	131.1	405.9	138.0	377.4	152.9	359.8	162.6	342.2	172.2
	9	462.1	116.8	439.6	128.0	430.1	132.6	416.2	139.4	386.9	154.4	368.8	164.1	350.7	173.8
	10	473.1	118.3	450.2	129.4	440.6	134.1	426.1	141.1	395.7	156.0	377.4	165.8	359.0	175.6
	12	495.6	121.2	471.5	132.6	461.7	137.2	446.4	144.1	414.8	159.4	395.4	169.3	375.9	179.2
	15	529.4	125.9	504.0	137.1	493.3	141.9	476.6	149.1	443.3	164.4	422.5	174.4	401.6	184.5

Table 2. Heat pump performance data in heating mode

Heating Capacities - AQTH STD/HSE/SIF - BLN Version

AQTH STD/HSE/SIF models	LWT (°C)	Ambient coil entering air temperature (°C)													
		-5		-3		0		5		7		10		15	
		Heat. cap. (kW)	Input power (kW)	Heat. cap. (kW)	Input power (kW)	Heat. cap. (kW)	Input power (kW)	Heat. cap. (kW)	Input power (kW)	Heat. cap. (kW)	Input power (kW)	Heat. cap. (kW)	Input power (kW)	Heat. cap. (kW)	Input power (kW)
1656 BLN	30	329.7	93.1	347.0	93.4	375.0	93.7	424.1	95.0	445.7	95.7	480.1	96.6	543.9	98.2
	35	325.4	109.5	345.7	104.5	372.8	104.8	419.8	106.1	440.5	106.8	473.7	107.7	534.4	109.5
	40	321.5	122.7	342.2	117.1	371.1	117.5	415.9	118.9	435.7	119.4	467.2	120.5	525.0	122.2
	45	318.1	138.0	338.3	131.6	366.8	132.1	412.5	133.3	431.0	134.0	461.2	134.9	515.5	136.8
	50					362.9	149.4	410.3	150.2	427.6	150.8	455.6	151.6	506.4	153.3

Table 3. Compressor partial load

Step t	1	2	3	4	5	6	7
p(%)	0	0,15	0,30	0,45	0,64	0,82	1

Condenser

The name condenser will be given to the heat exchanger of the system that plays the condenser role in heat pump mode and evaporator in the cooling mode. Indeed this component should normally be called evaporator in cooling unit mode, but to simplify the notation it will be called condenser without any considerations of the used mode (it is important to notice that the opposite convention is employed in the manufacture document [7]). This condenser is a “Dual Circuit” brazed stainless steel plate type heat exchanger. It allows heat exchanges between the refrigerant and water glycol circuit. The water glycol circulation is supported by a double pump that provides a constant flow rate (\dot{V}_w) of 88m³/h (obtained by calibrating the model to manufacturer data [7], [8]).

Evaporator

The same remark as for the condenser can be made for the use of “evaporator” name. Its coils are made of seamless copper tubes, arranged in staggered rows. It allows heat exchange between the refrigerant and the outside air.

Heat Pump Performance

The heat pump performance evaluation has to be evaluated throughout the all system life cycle, because it enables energy consumption estimation, optimization, lifetime commissioning. Usually we associate the heat pump performance to the coefficient of performance (*COP*). According to Carnot equations the theoretical equations for the *COP* are:

$$COP_{th,cold} = \frac{T_{cold}}{T_{hot} - T_{cold}}. \quad (1)$$

$$COP_{th,heat} = \frac{T_{hot}}{T_{hot} - T_{cold}}. \quad (2)$$

In our case, $T_{cold} = T_{out}$ and $T_{hot} = (T_{wout} - T_{win}) / 2$ (with T_{wout} and T_{win} the condenser leaving and return temperature, and T_{out} the outside temperature).

Nevertheless, in practice we define the *COP* of a heat pump as the division of the condenser load \dot{Q}_c by the compressor power \dot{W} . Without the convention taken about “condenser” and “evaporator” name, the heat pump mode used has to be considered. Indeed the *COP* in cold mode is equal to the load of the evaporator divided by the input compressor power. The compressor power \dot{W} and the condenser load \dot{Q}_c , can be define as explained in the following text:

Input compressor power \dot{W} , as explained in the work of Djuric et al. [8], about data fusion, can be estimating using direct and indirect measurements

The direct method required the knowledge of suction and discharge pressures and several constant parameters:

$$\dot{W}_d = \frac{1}{\eta} \cdot \frac{\gamma}{\gamma-1} \cdot \dot{V}_s \left[1 + C - C \left(\frac{P_{dis}}{P_{suc}} \right)^{1/\gamma} \right] P_{suc} \left[\left(\frac{P_{dis}}{P_{suc}} \right)^{(\gamma-1)/\gamma} - 1 \right] + \dot{W}_{loss}. \quad (3)$$

The indirect method uses the *Table 1* and *Table 2* and steps of circuit 1 and 2 in *Table 3*. Each step is related to the part load p of each circuit in *Table 3*. And in *Table 1* and *Table 2*, we can find the input compressor power in full load (in function of the outside temperature T_{out} and the condenser leaving temperature T_{wout}).

$$t = \frac{\dot{W}}{\dot{W}_{FL}}. \quad (4)$$

$$\dot{W}_{id} = t \cdot \dot{W}_{FL}(T_{out}, T_{wout}). \quad (5)$$

Condenser load \dot{Q}_c , can be also estimated using direct and indirect measurements. The direct measurement can be obtained using the water temperature difference:

$$\dot{Q}_{c,d} = \rho_w \cdot \dot{V}_w \cdot C_{pw} (T_{w,out} - T_{w,in}). \quad (6)$$

The indirect measurement is determined using the condenser load at full load $\dot{Q}_{c,FL}$ given in *Table 1* and *Table 2*, an additional model parameter UA of the heat exchanger (obtained by calibrating the model to the manufacturer data, as explained in [8]).

$$\dot{Q}_{c,id} = \frac{1 - \exp(-(UA_{cd,FL}/V_w \times C_{pw})t^m)}{1 - \exp(-(UA_{cd,FL}/V_w \times C_{pw}))} \cdot \dot{Q}_{c,FL}(T_{out}, T_{wout}). \quad (7)$$

Since there are two methods to estimate \dot{W} and \dot{Q}_c , direct and indirect, we can define a COP "direct" using the *Equation 8*, a COP "indirect" using the *Equation 9* and a COP "combined", if we used a combination of direct and indirect measurement for the condenser load and the input compressor power.

$$COP_d = \frac{\dot{Q}_{c,d}}{\dot{W}_d} = \frac{\rho \cdot \dot{V}_w \cdot C_{pw} (T_{w,out} - T_{w,in})}{\frac{1}{\eta} \cdot \frac{\gamma}{\gamma-1} \cdot \dot{V}_s \left[1 + C - C \left(\frac{P_{dis}}{P_{suc}} \right)^{1/\gamma} \right] P_{suc} \left[\left(\frac{P_{dis}}{P_{suc}} \right)^{(\gamma-1)/\gamma} - 1 \right] + \dot{W}_{loss}} \quad (8)$$

$$COP_{id} = \frac{\dot{Q}_{c,id}}{\dot{W}_{id}} = \frac{\frac{1 - \exp(-(UA_{cd,FL}/\dot{m}_w \cdot C_{pw})t^m)}{1 - \exp(-(UA_{cd,FL}/\dot{m}_w \cdot C_{pw}))} \cdot \dot{Q}_{c,FL}(T_{out}, T_{wout})}{t \cdot \dot{W}_{FL}(T_{out}, T_{wout})} \quad (9)$$

Parameters considered as constant are mentioned in the *List of symbols*.

In our case we can also define a manufacturer theoretical maximal COP using *Table 1* and *Table 2*. Regarding the air temperature T_{air} and the condenser leaving temperature T_{wout} , we can determine by extrapolation and interpolation the input compressor power and the condenser load in full load ($\dot{W}_{FL}(T_{out}, T_{wout})$ and $\dot{Q}_{c,FL}(T_{out}, T_{wout})$). Thus we obtain the following COP:

$$COP_{th,FL} = \frac{\dot{Q}_{c,FL}(T_{out}, T_{wout})}{\dot{W}_{FL}(T_{out}, T_{wout})} \quad (10)$$

Air Handling Unit

An air handling unit (AHU) is a device used to condition and circulate air as part of a HVAC system. An AHU is usually a large metal box containing fans, heating or cooling

elements, filter racks or chambers, sound attenuators, and dampers. An AHU is usually connected to ductwork that distributes the conditioned air through the building (or a part of it if several AHU are used, like our case) and returns it to the AHU. Contrary to a Constant Air Volume (CAV), for a VAV the air volume can be controlled. This is an important advantage since it enables a substantial reduce of fans energy consumption.

The AHU concerned by our studies and shown in *Figure 3*, has an air volume capacity of 15 000 m³/h. It is composed of a rotary heat recovery system, a supply damper, an exhaust damper, filters, two fans with a frequency regulator, a heating/cooling coil a heating coil.

The heating/cooling coil capacity is 63,28 kW and the heating coil capacity is 41,68 kW.

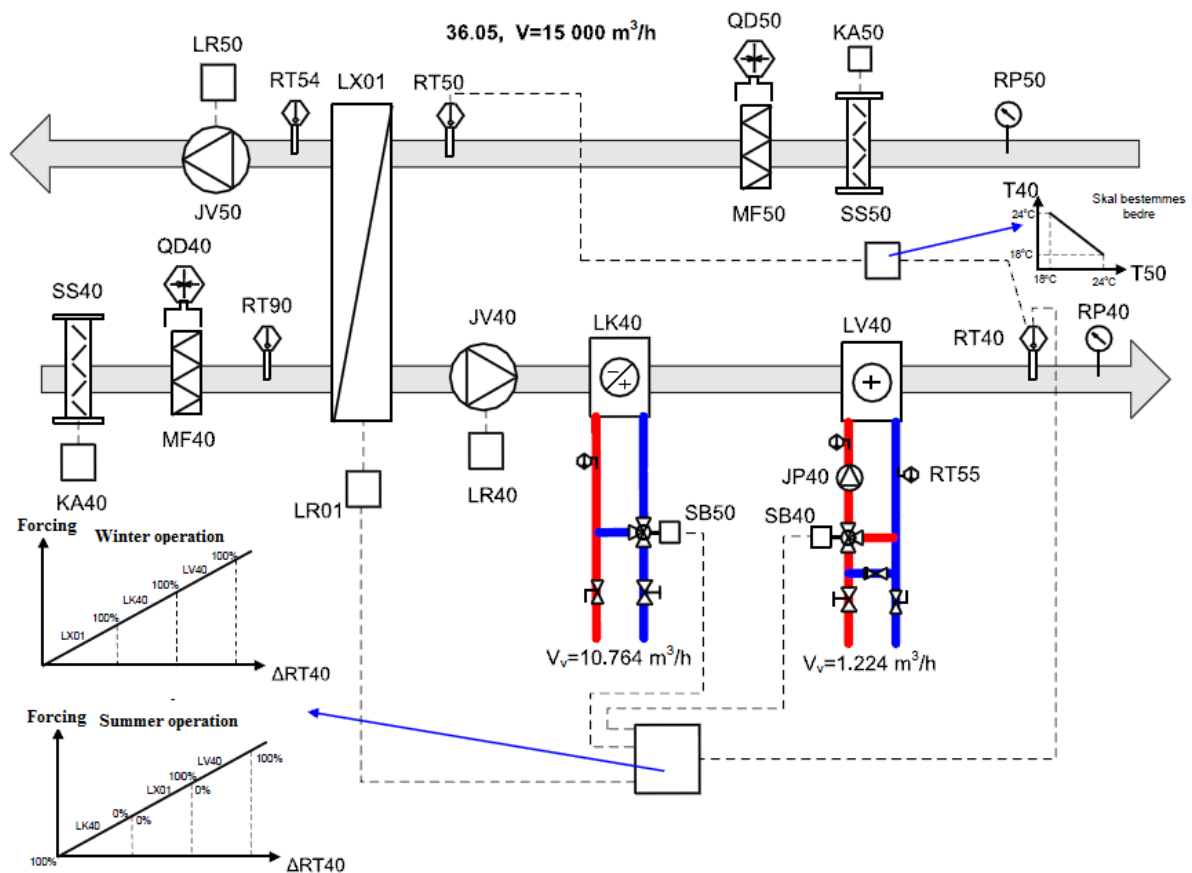


Figure 3. Schematic of Variable Air Volume Studied

Rotary Heat Recovery System

It is a slowly rotating matrix of finely corrugated metal, operating in both opposing airstreams. When the AHU is in heating mode, heat is absorbed as air passes through the matrix in the exhaust airstream (during one half rotation), and released into the supply airstream (during the second half rotation) in a continuous process. When the air handling unit is in cooling mode, heat is released as air passes through the matrix in the exhaust airstream, and absorbed into the supply airstream. Heat recovery efficiency is up to 85%. This efficiency increases with the wheel speed until a certain limit. Once this level is reached,

an increase of the wheel speed will not increase the system efficiency anymore. In our case the motor that makes turn the wheel has a power of 100 W.

The disadvantage of the rotary heat recovery system is the non tightness between supply and exhaust air stream. This problem is reduced by using brush seals and a small purge section (a little part of the supply air go into the exhaust conduct, avoiding the opposite).

Heating/Cooling Coil

This heat exchanger enables to heat or cool the air heat transfer from a mixture of water and glycol. The water glycol is circulating from the analyzed heat pump condenser. The air goes through aluminum brazed plates that are pierced by many tubes. The water glycol circulates in those tubes.

A three way diverting valve allows the control of the heat transfer. The maximal heat transfer power is 63.28 kW. In this kind of mounting, the water glycol temperature that arrives in the coil is constant, and equal to the water glycol temperature that leaves the heat pump. Heat losses in pipes were neglected because pipes are well isolated. The control on the heat input is made on the flow rate, as shown in *Figure 4*. The three way valve is control by the BEMS.

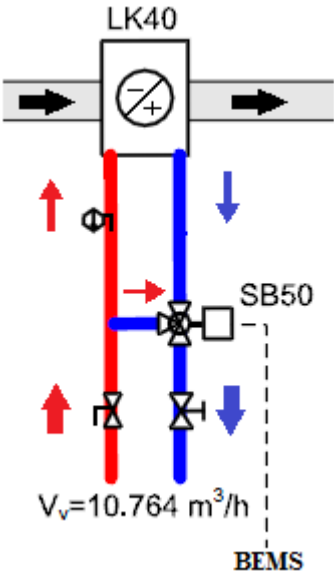


Figure 4. Heating/cooling coil

Heating Coil

The heating coil is the same kind of heat exchanger that the heating/cooling coil. But this time transfer fluid is water and is provided by district heating. The maximal heat transfer power is 41,68 kW. Moreover the three way valve is a mixing valve. The water flow rate that arrives in the coil is constant. The control is made on the temperature, by mixing inlet and outlet water as shown in *Figure 5*. The three way valve is controlled by supply air temperature.

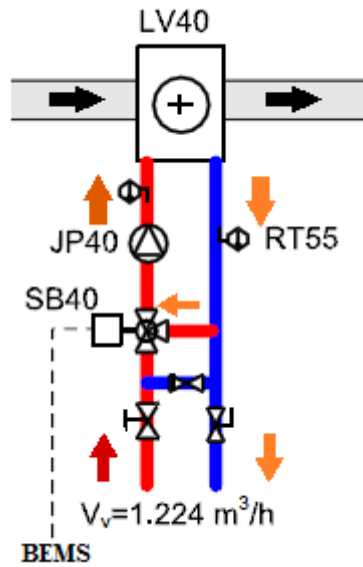


Figure 5. Heating coil

Three Way Valves

The three way valves have huge role in the control of the system studied. Also it is important to focus on the operation and characteristics of that component. As explained in ASHRAE Systems and Equipment Handbook 2000 [9], a valve is usually defined by its control range R given in Equation 11, its authority A given in Equation 12 and its control flow characteristic. R can have a value from 30 to 50, A can have a value from 0.3 to 0.7 and the control flow characteristic can be quick opening, linear or equal percentage.

$$R = \frac{\text{maximal flow rate}}{\text{minimal flow rate}} \quad (11)$$

$$A = \frac{\text{pressure drop of the fully open valve}}{\text{pressure drop of the fully open valve} + \text{system loop pressure drop}} \quad (12)$$

The authority A defines how the valve opening will contribute in changes in the system. In our case it determines how quickly the heat power transfer will increase with the valve opening. If A is too low (<0.3), the heat transfer power will be not negligible even in the zone of valve closing and it will reach quickly high values with valve opening (*almost 85% of maximal power heat transfer with an opening of 50% for a linear valve, see Figure 6*). Consequently it can be a problem for the system regulation. In the opposite if A is too high (>0.7), the pressure drop induced will be too important (*requirement of a more powerful circulator*).

Sometimes in practice, it can happen that documentation is lost. Therefore we do not know exactly the values of A and R . It is the case for our system.

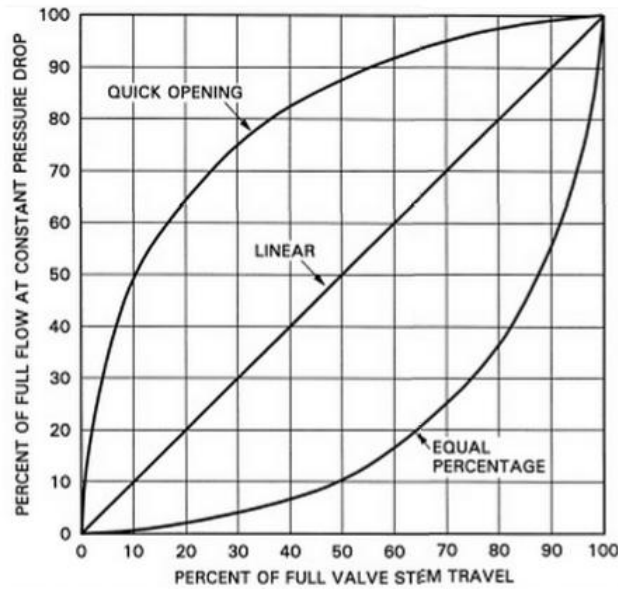


Figure 6. Control Valve Flow Characteristics

Generally, valves control the fluids flow rate thanks to an actuator, which moves a stem with an attached plug. Based on the geometry of the plug, we will have one of these three control flow characteristic shown in *Figure 6*:

- **Quick Opening:** When started from the closed position, a quick-opening valve allows a considerable amount of flow to pass for small stem travel. As the stem moves toward the open position, the rate at which the flow is increased per movement of the stem is reduced in a nonlinear fashion. This characteristic is used in two-position or on/off applications.

- **Linear:** Linear valves produce equal flow increments per equal stem travel throughout the travel range of the stem. This characteristic is used on steam coil terminals and in the bypass port of three-way valves. *Equation 13* defines the relation between the flow rate, the percentage of valve opening x (stem position) and valves characteristics R and A .

$$q = q_{max} \cdot x_p \quad \text{with } x_p = \frac{x+(1-x)/R}{\sqrt{(1-A \cdot [(x+(1-x)/R)^2 - 1])}} \quad (13)$$

- **Equal Percentage:** This type of valve produces equal heat output increments per equal stem travel throughout the travel range of the stem, when in the same time the flow increases exponentially as the stem moves from the closed to the open position (*Figure 7*). The term equal percentage means that for equal increments of stem travel, the flow increases by an equal percentage. For example, in *Figure 6*, if the valve moves from 50 to 70% of full stroke, the percentage of full flow changes from 10 to 25%, an increase of 150%. Then, if the valve moves from 80 to 100% of full stroke, the percentage of full flow changes from 40 to 100%, again, an increase of 150%. This characteristic is recommended for control on hot and chilled water terminals. *Equation 14* defines the relation between the flow rate, the percentage of valve opening x (stem position) and valves characteristics R and A .

$$q = q_{max} \cdot x_p \quad \text{with } x_p = \frac{R^{x-1}}{\sqrt{(1-A \cdot [R^{2 \cdot (x-1)} - 1])}} \quad (14)$$

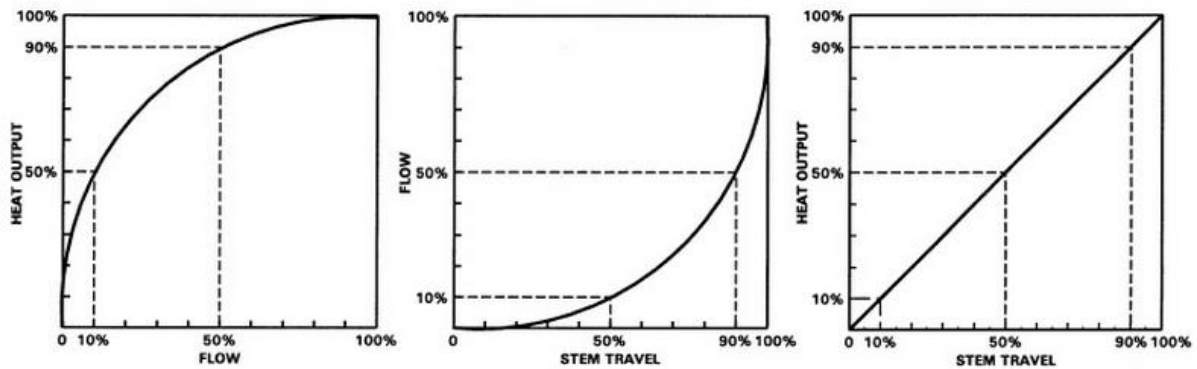


Figure 7. Heat Output, Flow, and Stem Travel Characteristics of Equal Percentage Valve

Available Data From The Monitoring System

Sensors in the system enable to have a view and record data. Notation for sensors is established based on labeling in BEMS. Sensors for the Heat pump and the district heating have respectively the prefix 35.01 and 32.01 and sensors for the AHU have the prefix 36.05.

Available sensors for the heat pump, district heating and AHU are the following:

Heat Pump and District Heating

- 35.01 RT50: Condenser water glycol inlet temperature, T_{win}
- 35.01 RT40: Condenser water glycol leaving temperature, T_{wout}
- 35.01 RT90: Outdoor temperature, T_{out}
- 32.01 RT40: District heating provided temperature, T_{LV-dh}
- 35.01 RP60: Discharge pressure circuit 1 (first group of 3 compressors), p_{dis1}
- 35.01 RP62: Suction pressure circuit 1, p_{suc1}
- 35.01 RP61: Discharge pressure circuit 2 (second group of 3 compressors), p_{dis2}
- 35.01 RP63: Suction pressure circuit 2, p_{suc2}
- Step circuit 1, $t1$
- Step circuit 2, $t2$
- Mode indicator (heat pump/cooling unit)
- State of water circulation pump (On/Off)

Air Handling Unit

- 36.05 RT90: Outdoor temperature, $T_{out}^{(1)}$
- 36.05 RT40: Supply air temperature, T_{sair}
- 36.05 RT40SPK: Supply air desired temperature, $T_{sair-des}$
- 36.05 RT50: Return Air temperature, T_{rair}
- 36.05 RT54: Return Air temperature after heat recovery system, T_{rair_hr}
- 36.05 RT55: Heating coil LV outlet water temperature, $T_{LV-wout}$
- 36.05 JV40: Supply fan signal, percentage of maximal supply air flow rate (x_{JV40})

- 36.05 JV50: Return fan signal, percentage of maximal return air flow rate, x_{JV50}
- 36.05 LX01: Heat recovery signal, percentage of maximal wheel speed, x_{LX01}
- 36.05 LK40: Three way valve signal of the Heating/Cooling coil, percentage of valve opening, x_{LK}
- 36.05 LV40: Three way valve signal of the Heating coil, percentage of valve opening, x_{LV}

- 36.05 RP40: Supply air pressure, p_{sup}
- 36.05 RP50: Return air pressure, p_{ret}

¹⁾: (There are two sensors for outdoor temperature. The sensor 35.01 RT90 will be used just in the case of heat pump COP calculations. In all other case T_{out} will refer to sensor 36.05 RT90).

Determination of the heat exchanged in each component

HVAC systems have a more and more huge role in the achievement of air indoor quality. In order to improve energy consumption, buildings are more and more isolated (thermal insulation, several glasses window, etc) and one of the most important big effect of that is the decrease of air infiltrations. Consequently the necessity of air renewal is less supported by natural ventilation, hence the greatest role of ventilation system in indoor air quality, thermal comfort and as an important source of energy consumption.

Here we are going to focus on the energy consumption and environmental aspects. In a first time the contribution of the heat recovery system and the two coils in the heat exchanged in our system will be determined. It will be a first step in optimization of control strategy. Indeed before optimization, heat demand of AHU will be estimated using few methods: Heat balance method, Valve position method and NTU method. These methods represent virtual measurements. They are based on BEMS signals introduced in the previous chapter. Moreover the methods developed might be also a way to highlight procedures that may be able to underscore sensors and signals faults.

BEMS data measured for March 2011 will be our training data to test these methods. However this data base contains outliers and missing values. Consequently a pre-processing is required to eliminate those issues in a first place. Indeed without any treatment those problems may corrupt the different methods results.

Pre-processing

Typical problems were found in the data base. Excel and Visual Basic macro are used to fix them. Their treatment procedures are explained further:

Missing values and outliers: The macro put a high value that will be considered as outlier in each empty cell. Then the outliers are treated as following: for each kind of parameters (pressure, temperatures, signal) a critical value has been defined.. Then for each column, the macro goes through all lines and compares each value with the critical value. When one of them is higher, it is replaced by the average of the previous value and the first next value which is not another outlier (comparison of the next values with the critical value until we are not dealing with an outlier).

Heat pump pressure signals equal to zero when partial load signal have a positive value: The compressor pressures of the heat pump are rarely equal to zero. Therefore, when it is the case, the macro looks at partial load signals. If the corresponding signal is positive, the pressure value is wrong. In this case the macro follow the same logic that outliers treatment (replacement of the value by an average value).

Partial load problems – sensors problems highlight: Sometimes the difference between the suction and discharge pressure seems to show that we are in a working time, but the corresponding partial load signal is equal to 0 (non working time). In this case outlier treatment is not possible. The origin of the problem is probably the partial load signal but its supposed value is unknown. Like partial load have finite value (see *Table 3*), we cannot calculate an average value as before.

However like many values in a row are concerned, this procedure enabled to highlight partial load signal problem.

Heat Balance Method

The purpose of this method is to estimate the heat exchanged in each component of our AHU: the heat recovery system, the heating/cooling coil and the heating coil.

The idea is quite simple. In a heat exchanger, the heat release by one fluid is gain by the other fluid, *Equation 15*. Also if we know the flow rate and the difference of temperature for one fluid, and the flow rate and just one temperature (inlet or outlet) for the other fluid, a heat balance allows to determine the missing temperature. More generally, on six variables (*flow rate of fluid one and fluid two, inlet temperature fluid one and fluid two, outlet temperature of fluid one and fluid two*) we need to know five of them (*plus physicals parameters of each fluids, such as heat capacity and eventually their density*).

$$\dot{V}_1 \cdot \rho_1 \cdot Cp_1 \cdot (T_{in\ 1} - T_{out\ 1}) = \dot{V}_2 \cdot \rho_2 \cdot Cp_2 \cdot (T_{out\ 2} - T_{in\ 2}) \quad (15)$$

Heat Recovery System, LX01

Regarding the rotary heat recovery system shown in the *Figure 8*, parameters provided by the BEMS are:

- The exhaust air temperature, T_{rair}
- The exhaust air temperature after heat recovery system, T_{rair_hr}
- The return fan signal, x_{JV50}
- The exhaust fan signal, x_{JV40}
- The outdoor temperature, T_{out}
- The air density, ρ_{air} and the air heat capacity, Cp_{air}

Some parameters are also given by the manufacturer data [10]:

- The maximal exhaust air flow rate, \dot{V}_{rair_max}
- The maximal supply air flow rate, \dot{V}_{sair_max}

The following physical parameters are also known:

- The air density, ρ_{air} and the air heat capacity, Cp_{air}

Finally there is just one missing value on the *Figure 8*: The supply air temperature after the heat recovery, T_{sair_hr} .

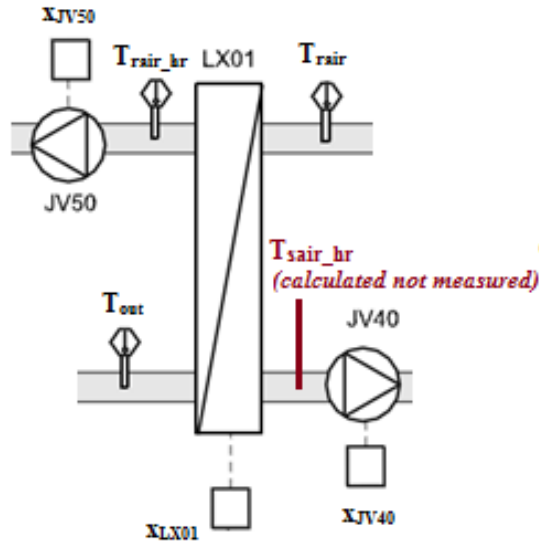


Figure 8. Rotary heat recovery system – heat balance

We use the heat balance described by Equation 16 to obtain T_{sair_hr} given in Equation 17).

$$x_{JV40} \cdot \dot{V}_{sair_max} \cdot \rho_{air} \cdot Cp_{air} \cdot (T_{sair_hr} - T_{out}) = x_{JV50} \cdot \dot{V}_{rair_max} \cdot \rho_{air} \cdot Cp_{air} \cdot (T_{rair} - T_{rair_hr}) \quad (16)$$

$$T_{sair_hr} = \frac{x_{JV50}}{x_{JV40}} \cdot (T_{rair} - T_{rair_hr}) + T_{out} \quad (17)$$

The heat exchanged in the heat recovery, \dot{Q}_{hr} is:

$$\dot{Q}_{hr} = x_{JV40} \cdot \frac{\dot{V}_{rair_max}}{3600} \cdot \rho_{air} \cdot Cp_{air} \cdot (T_{sair} - T_{sair_hr}) \quad (18)$$

Heating Coil, LV

Regarding the heating coil LV shown in Figure 9, parameters provided by the BEMS are:

- The supply air temperature, T_{sair}
- The supply air flow rate (equal to $\dot{V}_{sair_max} \times x_{JV40}$)
- The heating coil outlet water temperature, T_{LV_wout}
- The district heating supply temperature, T_{LV_dh}
- Three way valve position signal of the Heating coil, x_{LV}

The only parameters given by the manufacturer data [10] is

- The water flow rate in the coil, \dot{V}_{LV} . It is a constant value

The following physical parameters are also known:

- The air and water density, ρ_{air} and ρ_w
- The air and water heat capacity, Cp_{air} and Cp_w

In this case there are two unknown values: $T_{\text{sair_LK}}$ and $T_{\text{LV_win}}$.

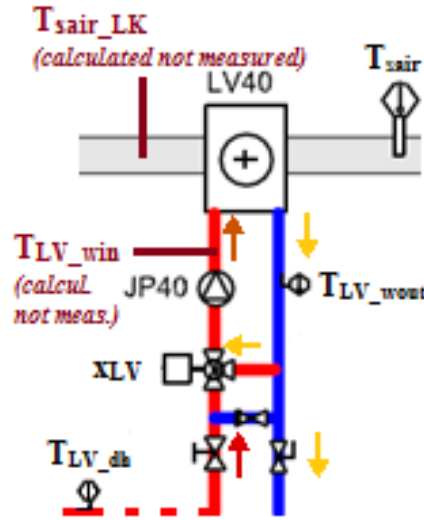


Figure 9. Heating coil – heat balance/valve equation

Information about the three way valve are required: values of R and A , and valve characteristic. Unfortunately these information are missing. Also, considering three way valves theories, the following hypotheses will be considered in a first time:

$$R = 40 ;$$

$$A = 0.4 ;$$

Valve characteristic: proportional

As there are two unknown parameters in our system, a heat balance equation cannot directly be used. However we know that the heating coil inlet water flow is a mixed of the heating coil outlet water flow and the district heating flow. Its flow rate is constant, equal to \dot{V}_{LV} , but its temperature $T_{\text{LV_win}}$ depends on the proportion of the flow coming from district heating and the outlet flow (*see explanation about the Heating Coil and especially mixing valve*). As we considered the valve characteristic as proportional, this proportion can be determined with the parameter x_p (rename $x_{\text{LV},p}$ in this case) of Equation 14. The following relation is obtained:

$$\dot{V}_{LV} = x_{\text{LV},p} \cdot \dot{V}_{LV} + (1 - x_{\text{LV},p}) \cdot V_{LV} \quad (19)$$

Then an enthalpy balance enables to determine the missing temperature $T_{\text{LV_win}}$:

$$\dot{V}_{LV} \times \rho_w \cdot C_{p_w} \times T_{\text{LV_win}} = x_{\text{LV},p} \dot{V}_{LV} \times \rho_w \cdot C_{p_w} \times T_{\text{LV_dh}} + (1 - x_{\text{LV},p}) V_{LV} \times \rho_w \cdot C_{p_w} \times T_{\text{LV_wout}} \quad (20)$$

$$T_{\text{LV_win}} = \frac{x_{\text{LV},p} \cdot \dot{V}_{LV} \cdot T_{\text{LV_dh}} + (1 - x_{\text{LV},p}) V_{LV} \cdot T_{\text{LV_wout}}}{\dot{V}_{LV}} \quad (21)$$

Once T_{LV_win} is known, a heat balance equation between the air and the water can be used to determine T_{air_LK} :

$$x_{JV40} \cdot \dot{V}_{sair_max} \cdot \rho_{air} \cdot Cp_{air} \cdot (T_{sair} - T_{sair_LK}) = \dot{V}_{LV} \cdot \rho_w \cdot Cp_w \cdot (T_{LV_win} - T_{LV_wout}) \quad (22)$$

$$T_{sair_LK} = T_{sair} - \frac{\dot{V}_{LV} \cdot \rho_w \cdot Cp_w \cdot (T_{LV_win} - T_{LV_wout})}{x_{JV40} \cdot \dot{V}_{sair_max} \cdot \rho_{air} \cdot Cp_{air}} \quad (23)$$

The heat exchanged in the heating coil calculated with this method, \dot{Q}_{LV_hb} is:

$$\dot{Q}_{LV_hb} = x_{JV40} \cdot \frac{\dot{V}_{rair_max}}{3600} \cdot \rho_{air} \cdot Cp_{air} \cdot (T_{sair} - T_{sair_LK}) \quad (24)$$

Heating/Cooling Coil, LK

Regarding the heating/cooling coil LK shown in *Figure 10*, parameters provided by the BEMS are:

- The supply air flow rate (equal to $\dot{V}_{sair_max} \cdot x_{JV40}$)
- The heating coil inlet water temperature, T_{LK_win} that is equal to the heat pump condenser leaving temperature T_{wout} .
- The three way valve position signal of the Heating/cooling coil, x_{LK}

The only parameters given by the manufacturer data [10] is

- The water flow rate before the three way valve, \dot{V}_{LK_max} (constant value)

The following physical parameters are also known:

- The air and water density, ρ_{air} and ρ_w
- The air and water heat capacity, Cp_{air} and Cp_w

As shown in *Figure 10*, there are four unknown values in this case. It is too many to use a heat balance method to calculate them.

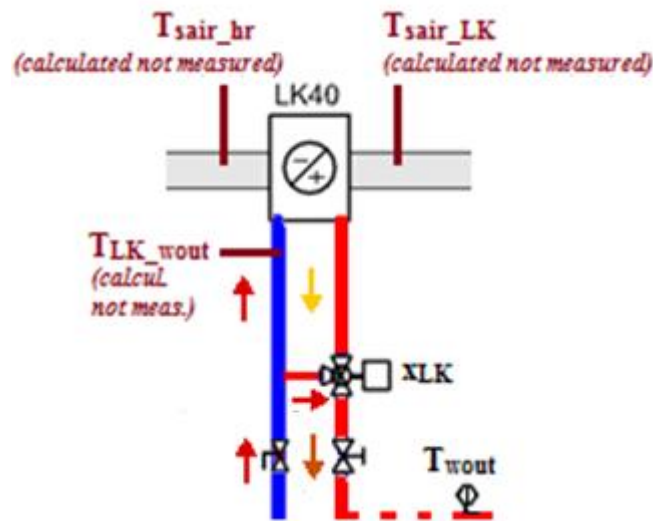


Figure 10. Heating/Cooling coil – heat balance/valve equation

Information about the three way valve are also missed for this coil. Consequently the same hypotheses that for the heating coil will be considered:

$$R = 40 ;$$

$$A = 0.4 ;$$

Valve characteristic: proportional

Whereas a heat balance method cannot be used for this coil, since the air temperature of the both side of this coil, T_{sair_hr} and T_{sair_LK} have already been calculated, the heat exchanged in this coil can be calculated as:

$$\dot{Q}_{LK_hb_air} = x_{JV40} \cdot \frac{\dot{V}_{rair_max}}{3600} \cdot \rho_{air} \cdot Cp_{air} \cdot (T_{sair_LK} - T_{sair_hr}) \quad (25)$$

At present T_{LK_wout} can be calculated by following the method developed to calculate T_{LV_win} for the heating coil. This time the water inlet temperature is known but not the water flow rate in the coil \dot{V}_{LK} . It can be determined with *Equation 14* (as previously we rename x_p by $x_{LK,p}$):

$$\dot{V}_{LK} = x_{LK,p} \cdot \dot{V}_{LK_max} \quad (26)$$

Then the missing temperature T_{LV_wout} can be calculated as follow with a heat balance:

$$x_{JV40} \cdot \dot{V}_{sair_max} \cdot \rho_{air} \cdot Cp_{air} \cdot (T_{sair_LK} - T_{sair_hr}) = \dot{V}_{LK} \cdot \rho_{wg} \cdot Cp_{wg} \cdot (T_{LK_win} - T_{LK_wout}) \quad (27)$$

$$T_{LK_out} = T_{LK_win} - \frac{x_{JV40} \cdot \dot{V}_{sair_max} \cdot \rho_{air} \cdot Cp_{air} \cdot (T_{sair_LK} - T_{sair_hr})}{\dot{V}_{LK} \cdot \rho_{wg} \cdot Cp_{wg}} \quad (28)$$

Finally, the heat exchanged in the heating/cooling coil can be calculated, but this time with the water side ($\dot{Q}_{LK_hb_wat}$) (*we did not do it for the heating coil, because it was the base of our calculation. Consequently we would have obtained the same value that \dot{Q}_{LV_hb}*):

$$\dot{Q}_{LK_hb_wat} = \dot{V}_{LK} \cdot \rho_{wg} \cdot Cp_{wg} \cdot (T_{LK_win} - T_{LK_wout}) \quad (29)$$

Valve Position Method

The purpose of this method is to evaluate the heat exchanged in the two coils by another way. This method cannot be applied for the heat recovery system.

This method uses the fact that heat exchanged in coils is directly linked (linear relation) to valve position, if three way valves have an equal percentage characteristic, as shown by *Figure 7*.

As we made the assumption that our valves have a proportional characteristic, the heat exchanged in each coil, \dot{Q}_{LK_x} and \dot{Q}_{LV_x} can be estimated by multiplying their position

signal by their maximal heat power exchanged. These powers are given in the manufacturer data [10].

$$\dot{Q}_{LK_x} = x_{LK} \cdot \dot{Q}_{LK_{max}} \quad (30)$$

$$\dot{Q}_{LV_x} = x_{LV} \cdot \dot{Q}_{LV_{max}} \quad (31)$$

NTU Method

Number of Transfer Unit (NTU) method is used to calculate the rate of heat transfer in heat exchangers, especially when two temperatures (among the four) are unknown (*Equation 15*). The NTU is representative of the exchange capacity of the exchanger and as a consequence linked to the heat exchanger efficiency η .

The NTU is equal to the dimensionless ratio (*Equation 32*):

$$NTU = \frac{hS}{\dot{V}c_{min}} \quad (32)$$

With h the global heat transfer coefficient of the exchanger, S the exchange area. $\dot{V}c_{min}$ is defined as follow. For the both fluid implied in the exchange, $\dot{V}c_1$ and $\dot{V}c_2$ are obtained by multiplying the fluid mass flow rate by its heat capacity. Then $\dot{V}c_1$ and $\dot{V}c_2$ are compared and the minimum will be $\dot{V}c_{min}$ and the maximum $\dot{V}c_{max}$. $\dot{V}c_{min}$ is the control fluid of the transfer.

With $\dot{V}c_1 < \dot{V}c_2$ and (fluid one =hot fluid, fluid two = cold fluid) we define the ratio z and the heat efficiency η as follow:

$$z = \frac{\dot{V}c_1}{\dot{V}c_2} \quad (33)$$

$$\eta = \frac{T_{in1} - T_{out1}}{T_{in1} - T_{in2}} \quad (34)$$

If the both fluids are not brewed in the heat exchanger, the following expression is also available:

$$\eta = 1 - \exp \left[\frac{\exp(-z \cdot NTU^{0.78}) - 1}{z \cdot NTU^{-0.22}} \right] \quad (35)$$

In the manufacturer data [10] the value of S can be found and then h can be determined with the condition of exchange given (still in the manufacturer data. Indeed maximal coils powers of heat exchanged are given with inlet and outlet temperatures) and thanks to this relation:

$$Power\ of\ heat\ exchanged = h \cdot S \cdot LMDT \quad (36)$$

$$\text{where } LMDT = \frac{(T_{out1} - T_{in2}) - (T_{in1} - T_{out2})}{\ln \left(\frac{(T_{out1} - T_{in2})}{(T_{in1} - T_{out2})} \right)} \quad (37)$$

Regarding the heating coil, as explained previously (heat balance method – *Heating Coil*, LV) we know the both flow rate (air and water) without any consideration of the valve position. First the control fluid is determined by the comparison of each $\dot{V}c$ and the determination of $\dot{V}c_{min}$ and $\dot{V}c_{max}$.

Then the NTU can be calculated with *Equation 32*, z with *Equation 33* and η with *Equation 35*. Finally a system of two equations is used to determine the heating coil inlet water temperature T_{LV_win} and the supply air temperature before the heating coil T_{sair_LK} . Those equations are a heat balance (*Equation 15*) and the coil efficiency determine using temperatures (*Equation 34*). Regarding which fluid is the control fluid we will have, if this is the air (in red missing values):

$$\left\{ \begin{array}{l} \eta = \frac{T_{sair_LK} - T_{sair}}{T_{sair_LK} - T_{LV_win}} \\ x_{JV40} \cdot \dot{V}_{sair_max} \cdot \rho_{air} \cdot Cp_{air} \cdot (T_{sair} - T_{sair_LK}) = \dot{V}_{LV} \cdot \rho_{wg} \cdot Cp_{wg} \cdot (T_{LV_win} - T_{LV_wout}) \end{array} \right. \quad (38)$$

$$(22)$$

We obtain:

$$\left\{ \begin{array}{l} T_{sair_LK} = \frac{\eta \cdot T_{LV_win} - T_{sair}}{\eta - 1} \\ T_{LV_win} = \frac{x_{JV40} \cdot \dot{V}_{sair_max} \cdot \rho_{air} \cdot Cp_{air} \cdot T_{sair} \cdot \left(\frac{1}{\eta - 1} - 1 \right) - \dot{V}_{LV} \cdot \rho_{wg} \cdot Cp_{wg} \cdot T_{LV_wout}}{\left[\frac{\eta \cdot x_{JV40} \cdot \dot{V}_{sair_max} \cdot \rho_{air} \cdot Cp_{air}}{1 - \eta} - \dot{V}_{LV} \cdot \rho_{wg} \cdot Cp_{wg} \right]} \end{array} \right. \quad (39)$$

$$(40)$$

If this is the water:

$$\left\{ \begin{array}{l} \eta = \frac{T_{LV_win} - T_{LV_wout}}{T_{LV_win} - T_{sair_LK}} \\ x_{JV40} \cdot \dot{V}_{sair_max} \cdot \rho_{air} \cdot Cp_{air} \cdot (T_{sair} - T_{sair_LK}) = \dot{V}_{LV} \cdot \rho_{wg} \cdot Cp_{wg} \cdot (T_{LV_win} - T_{LV_wout}) \end{array} \right. \quad (41)$$

$$(22)$$

We obtain:

$$\left\{ \begin{array}{l} T_{LV_win} = \frac{\eta \cdot T_{sair_LK} - T_{LV_wout}}{\eta - 1} \\ T_{sair_LK} = \frac{\dot{V}_{LV} \cdot \rho_{wg} \cdot Cp_{wg} \cdot T_{LV_wout} \cdot \left(\frac{1}{\eta - 1} - 1 \right) - x_{JV40} \cdot \dot{V}_{sair_max} \cdot \rho_{air} \cdot Cp_{air} \cdot T_{sair}}{\left[\frac{\eta \cdot \dot{V}_{LV} \cdot \rho_{wg} \cdot Cp_{wg}}{1 - \eta} - x_{JV40} \cdot \dot{V}_{sair_max} \cdot \rho_{air} \cdot Cp_{air} \right]} \end{array} \right. \quad (42)$$

$$(43)$$

We do not have enough known values to apply this method to the heating/cooling coil. Also, instead of using this method to determine the missing air temperatures, they will be defined as follow:

- The coil inlet air temperature will be the supply air temperature after the heat recovery calculated with heat balance method.

- The coil outlet air temperature will be the supply air temperature after heating/cooling coil calculated with NTU method applied to the heating coil

Finally the heat exchanged in the both coils \dot{Q}_{LK_NTU} and \dot{Q}_{LV_NTU} is estimated as previously with *Equation 24 and 25*.

Combination of the NTU and valve position methods

This method is not relevant in our case, as we have serious doubts about the quality of valves signals (this fact will be explained in results interpretations), but even if we had good measured data, another problem can occur with the valve position method: the maximal power of the heat exchanger. Indeed this power is given by the manufacturer, but for specific temperatures and flow rate. Also if we are not close to these values, the real maximal power of the heat exchanger can be different.

The NTU method enables to recalculate this maximal power for each configuration of temperatures and flow rates. For example for the heating coil, we consider the valve fully open. Thus the water inlet temperature T_{LV_win} is known (equal to the district heating supply temperature T_{LV_dh}). And thanks to the relation between the heat exchanger efficiency η and inlet/ outlet temperatures of the fluids (Equation 34), the new water outlet temperature T_{LV_wout} can be calculated. Finally the heat power exchanged has to be determined. As the valve was considered fully open, this power will be equal to the theoretic maximal heat power exchanged. (In this case it is also possible to apply this method to the heating/cooling coil). Once we have the recalculated maximal heat power exchanged in each coil, the valve position method can be applied (multiplication of the valve signal by those powers).

Principal Component Analyses (PCA) method

In the project thesis related to this master thesis [6] we used the Principal Component Analysis (PCA) method [11] to highlight sensor faults in the heat pump system.

Principal Component Analysis (PCA) is a bilinear modeling method that uses an orthogonal transformation. It enables to convert the original variables, which are supposed to be correlated, into a new set of uncorrelated variables, which are called principal component. The number of principal components is less than or equal to the number of original variables.

Each PC explains a certain amount of the total information contained in the original data. The first PC contains the greatest source of information in the data set. Each subsequent PC contains, in order, less information than the previous one. By plotting PCs important sample and variable interrelationships can be revealed, leading to the interpretation of certain sample groupings, similarities or differences.

Many types of plots can be use to interpret and to optimize a PCA: explained variance, variances and RMSEP, scores, influence, variable residuals [12], [13]. But here we will just use the variable residuals.

Variable residuals: This is a plot of residuals for a specified X-variable and component number for all the samples. The plot is useful for detecting outlying sample/variable combinations. Also, once a sensor fault is detected, this plot may help to find which sensor is implied. In our case we will use it to regard the quality of measurement.

Results Interpretations

Heat Balance/ Valve Position/ NTU methods Comparison

Regarding heat balance, valve position and NTU methods, we obtained the results shown in *Figure 11* and *Figure 12*:

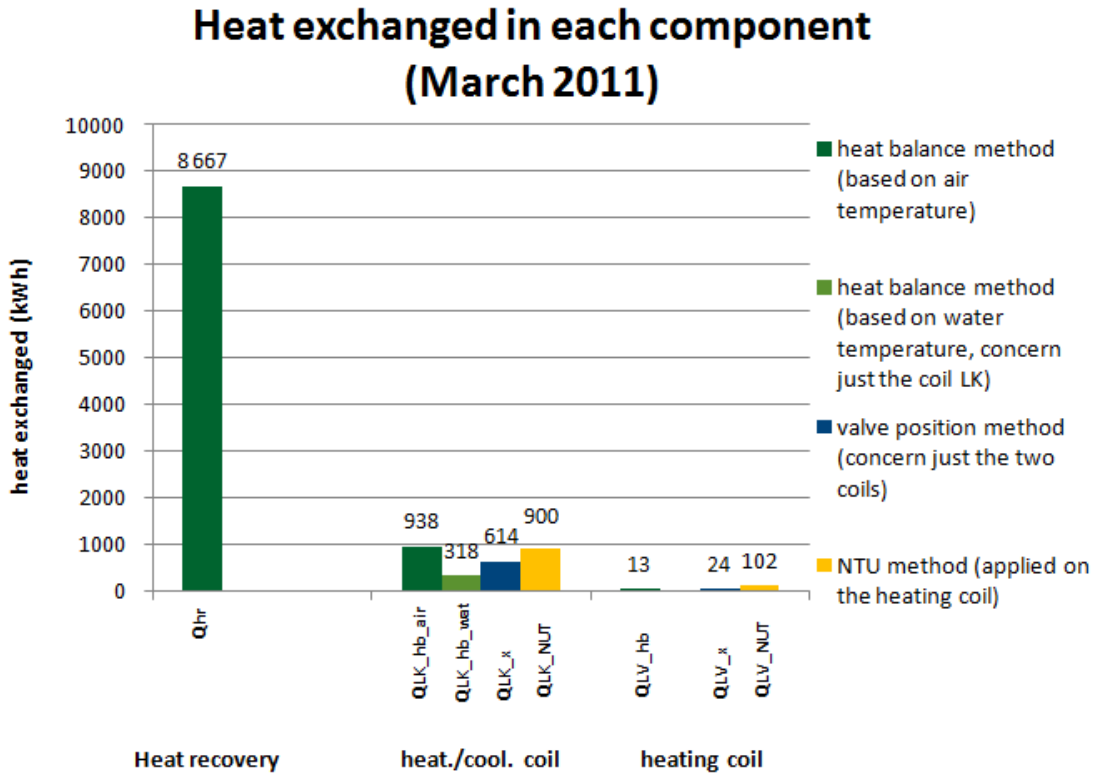


Figure 11. Total heat exchanged in each component during March 2011 determined with proposed methods

Heat exchanged in each component (March 2011)

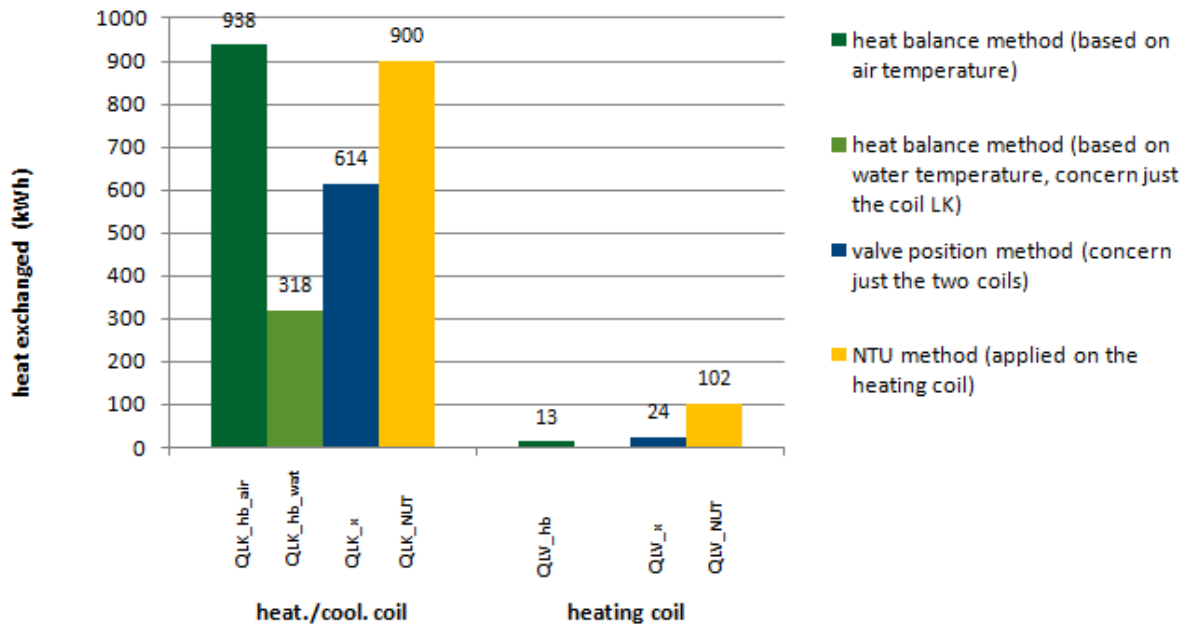


Figure 12. Total heat exchanged in the two coils during March 2011 determined with heat balance, valve position and NTU methods

Regarding the heat balance method, the first observation we can make is the big difference of the heat exchanged in the heating/cooling coil calculated on air and water (66%). Indeed, in many cases our calculation showed a difference of temperature before and after the coil, when in the same time the water flow rate in it was supposed to be zero.

Another issue is the difference between the heat balance method and the valve position method results. For the heating/cooling coil we have a difference of 35% between the two methods (heat balance method based on air temperature) and 55% (heat balance method based on water temperature). For the heating coil we have a difference of 28% between the two methods.

Regarding the heating/cooling coil, the difference between the NTU method and the heat balance method (based on air temperature) is only 4%. But in the same time, for the heating coil, the difference between NTU and balance methods is equal to 86%. Consequently we cannot say that the two methods give equivalent results. This is also confirmed by *Figure 13* that give the heat exchanged in the heating coil calculated on minute basis with the valve position method and the NTU method:

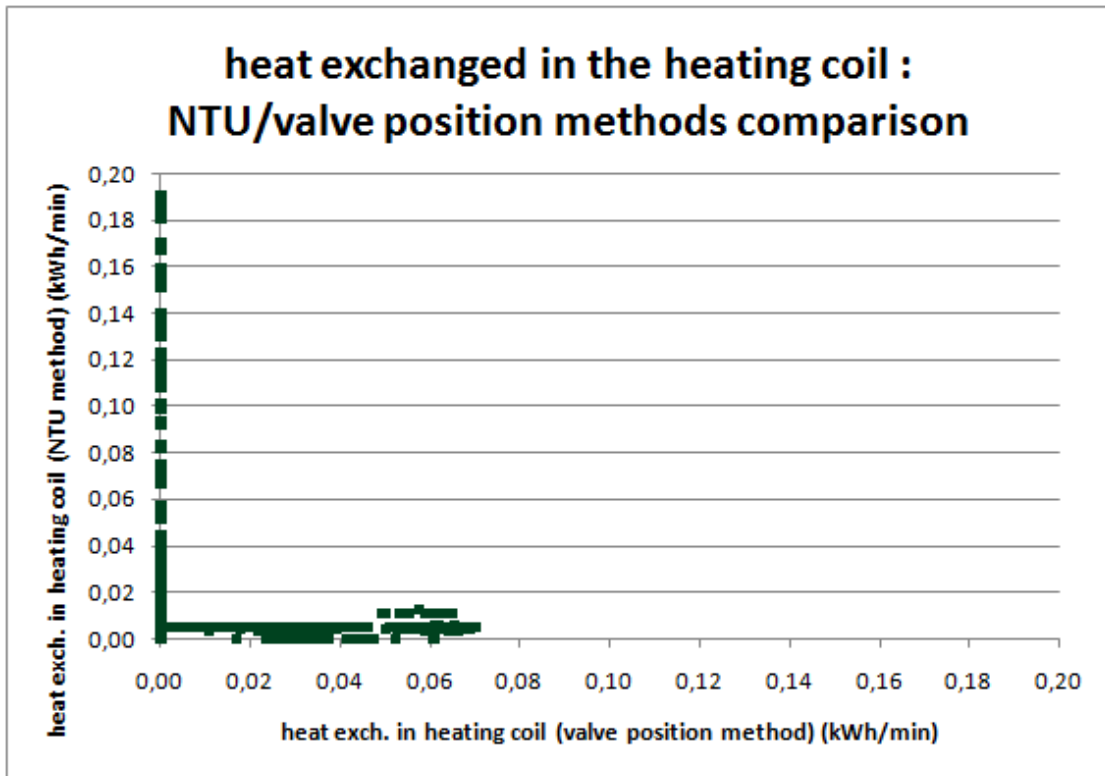


Figure 13. Heat exchanged in the heating coil: NTU /valve position methods (minute basis)

Comparison between the heat exchanged in the heating/cooling coil calculated on minute bases with the heat balance method (based on air temperature) and the valve position method is shown in *Figure 14* :

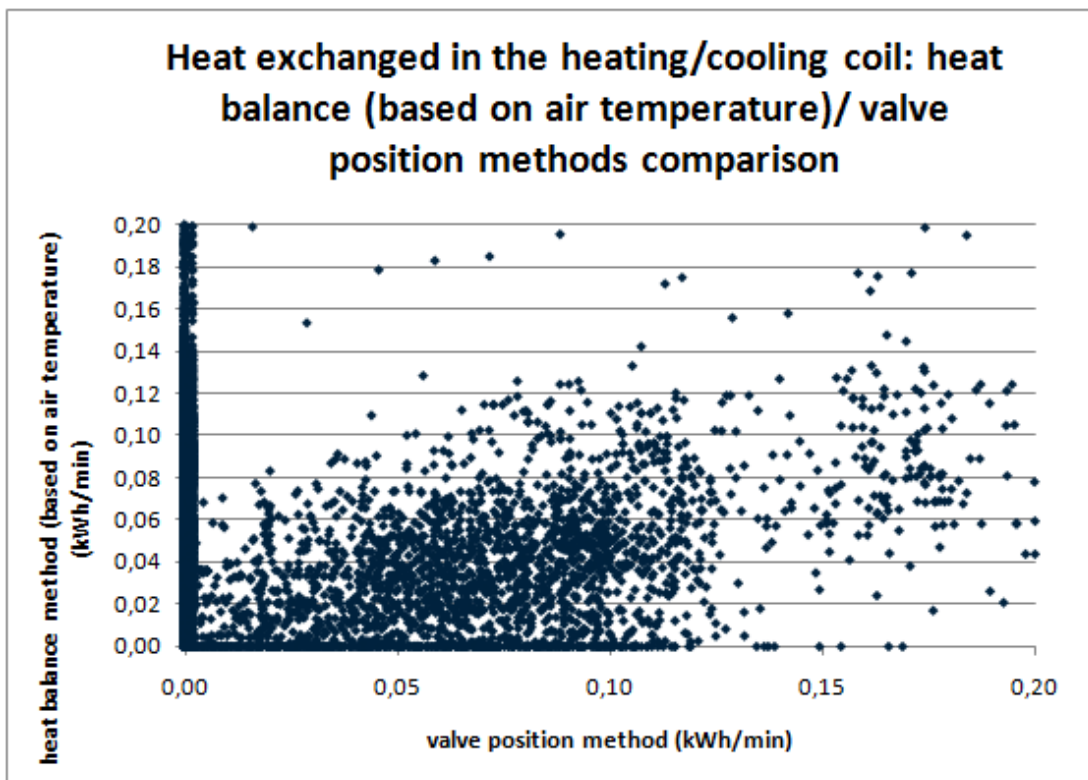


Figure 14. Heat exchanged in the heating/cooling coil heat balance (based on air temperature)/valve position methods (minute basis)

Several reasons can explain results shown in *Figure 14*. Firstly, we made hypotheses on valve characteristics (proportional or linear) and valve parameters values (A and R). Those hypotheses could be wrong.

Also we remade our calculation with several other configurations. The results of this model sensity analysis are presented in *Table 4* :

heating/cooling coil valve			heating coil valve			heat exchanged								
charact.	A	R	charact.	A	R	Q_LK_hb_Air (kWh)	Q_LK_hb_Wat (kWh)	Q_LK_hb_Air / Q_LK_hb_Wat difference	Q_LK_x (kWh)	Q_LK_hb_Air / Q_LK_x difference	Q_LK_hb_Wat / Q_LK_x difference	Q_LV_hb (kWh)	Q_LV_x (kWh)	Q_LV_hb / Q_LV_x difference
prop.	0,5	40	prop.	0,5	40	939,83	319,60	66%	614,26	35%	48%	10,85	24,24	55%
prop.	0,3	30	prop.	0,3	30	937,93	317,76	66%	614,26	35%	48%	14,30	24,24	41%
prop.	0,8	50	prop.	0,8	50	941,27	320,99	66%	614,26	35%	48%	8,60	24,24	65%
prop.	0,3	50	prop.	0,3	50	940,49	320,23	66%	614,26	35%	48%	9,81	24,24	60%
prop.	0,8	30	prop.	0,8	30	938,94	318,74	66%	614,26	35%	48%	12,42	24,24	49%
linear	0,5	40	linear	0,5	40	934,12	314,04	66%				31,88		
prop.	0,5	40	linear	0,5	40	938,94	318,74	66%	614,26	35%	48%	12,42		
linear	0,5	40	prop.	0,5	40	933,90	313,87	66%				33,35	24,24	27%
prop.	0,8	50	linear	0,8	50	934,12	314,04	66%	614,26	34%	49%	31,88		
linear	0,8	50	prop.	0,8	50	941,27	320,99	66%				8,60	24,24	65%

Table 4. Valves characteristics and parameters influence on Heat balance and valve position methods

For the heating/cooling coil, the different configurations do not change at all the difference between results obtained with the different methods. For the heating coil we can see some changes, but they are not relevant considering the low values of heat exchanged.

Consequently we cannot figure if our hypotheses were good or not, but they do not seem to be involved in the difference we obtained. We have to find another explanation.

Unfortunately the principal other reason that could provoke such difference, is a measurement uncertainty and especially a problem with valves signals. Results on *Figure 13* are consistent with that. Indeed when we have a lot of points for which the NTU method give a non negligible value, whereas the valve position method give always very low value (and even zeros values).

PCA Applied On The Air Handling Unit Sensors

PCA method is a way to verify the valves positions signals quality and therefore confirm or not our hypothesis about their poor quality. In this purpose PCA is used with all the Air Handling Unit sensors previously presented (*Available Data From The Monitoring System*) for measured data of March 2011. A focus is made on variable residuals plot.

We obtain the figures below:

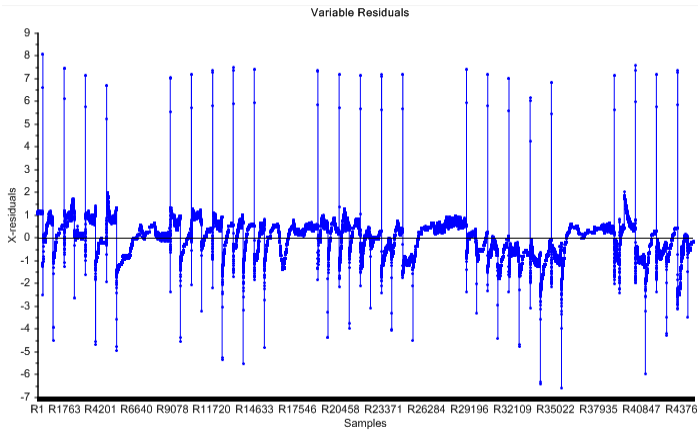


Figure 15. LX01 – x_{LX01} , Q-residuals (PC3)

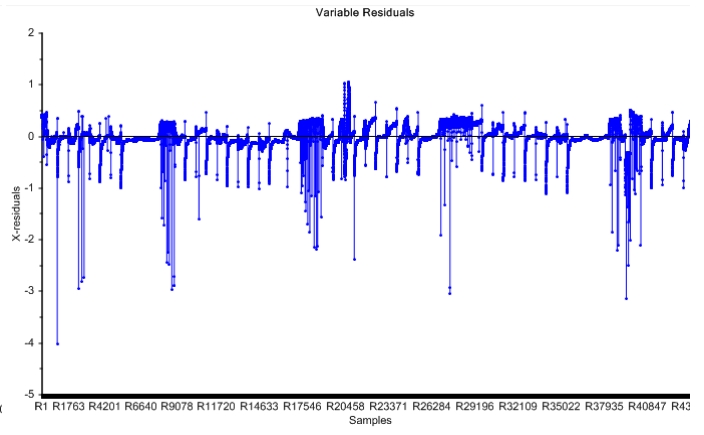


Figure 16. LK40 – x_{LK40} , Q-residuals (PC3)

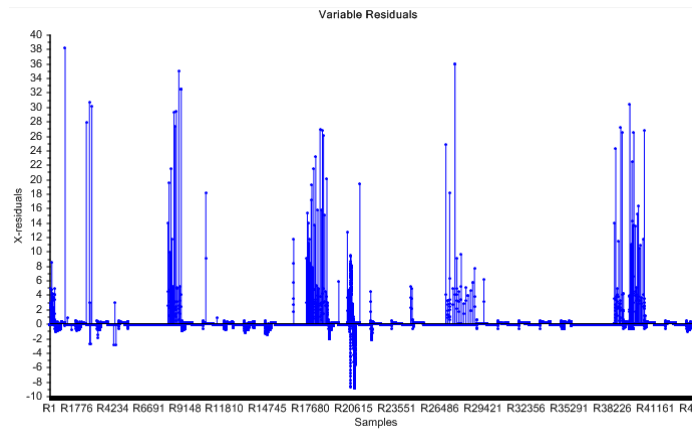


Figure 17. LV40 – x_{LV40} , Q-residuals (PC3)

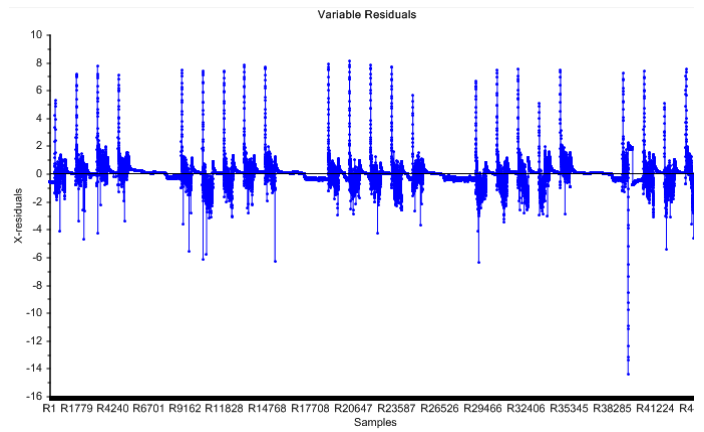


Figure 18. JV40 – x_{JV40} , Q-residuals (PC3)

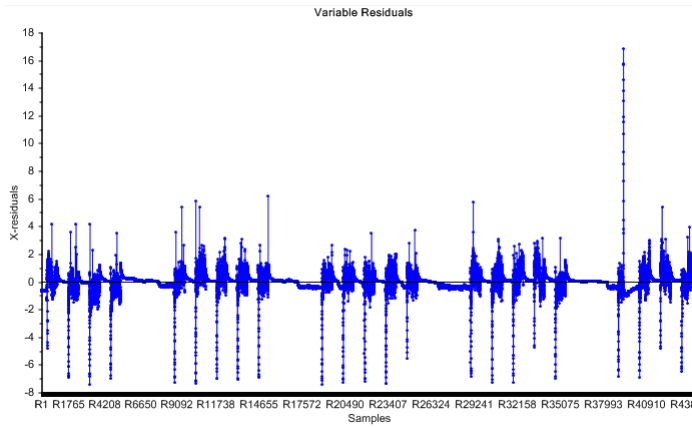


Figure 19. JV50 – x_{JV50} , Q-residuals (PC3)

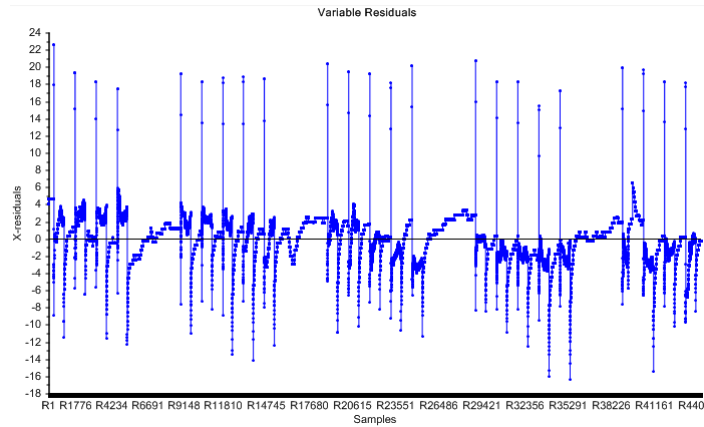


Figure 20. RT90 – T_{out} , Q-residuals (PC3)

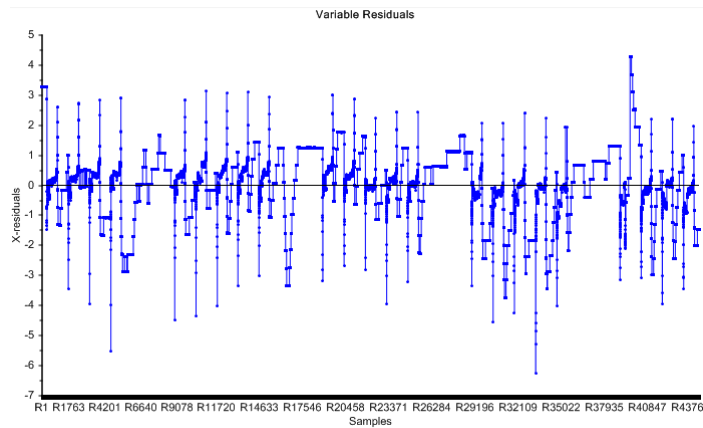


Figure 21. RT50 - T_{rairr} Q-residuals (PC3)

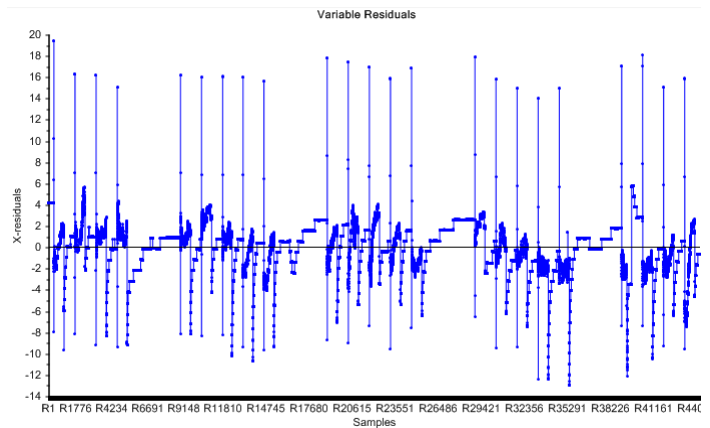


Figure 22. RT54 - T_{rair_hrr} Q-residuals (PC3)

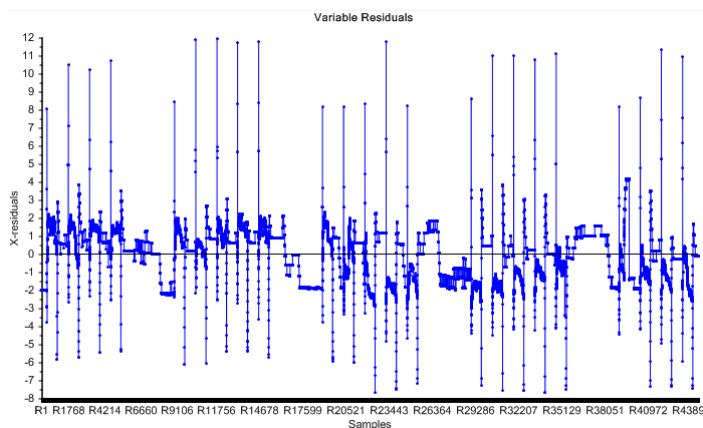


Figure 23. RT40 - T_{sairr} Q-residuals (PC3)

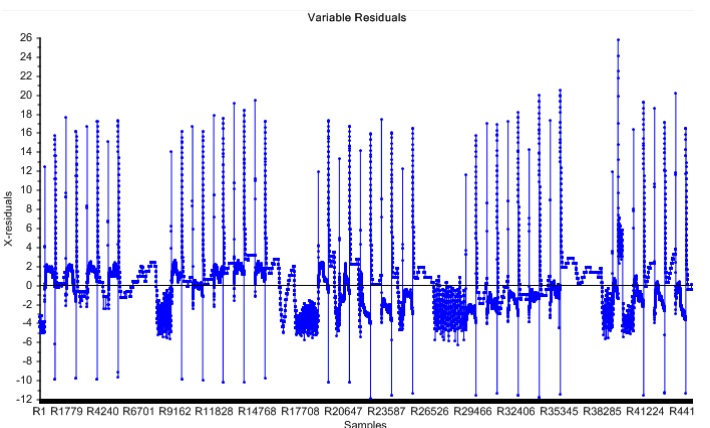


Figure 24. RT55 - T_{LV_woutrr} Q-residuals (PC3)

Almost all the variable residuals plot have periodic outliers. It seems to describe the launch of the system in working days. Indeed each series is composed of five outliers, then there is "blank" without any outliers, week-end, and again a set of five outliers. As a consequence we can think that those outliers are induced by the start of the system in working days. They can be explained by a different response time between sensors.

Nevertheless this observation is not valuable for two sensors: the valves position signals (Figure 16 and Figure 17). Q-residuals plot of these two signals contains many outliers and contrary to other plots, they are not periodic. Thus the PCA method applied in our case is consistent with our hypothesis: valves positions signals have a poor quality.

We can remark that the addition of a temperature sensor between the two coils would be a quicker way to highlight this kind of issue.

Optimization of control strategy in AHU

Our purpose is to optimize the control strategy of the AHU studied in order to decrease the energy costs and/or the CO₂ emissions induced by the use of this AHU. To achieve this goal, we will work on new distributions between components of the heat provided, when the total heat provided will stay the same for each method in order to make available comparison. Therefore it is necessary to know the contribution of each component minute by minute. This aim was the purpose of the last part, with development of methods that allow these estimations.

Due to problems with the valves position signals, we have not been able to validate proposed methods. However, the NTU method is the only one that does not use at all the valves signals. Consequently we will use the results obtained with this method in our approach.

Current control rules

Before proposing optimization of control strategy, it is necessary to define the current control strategy.

The control strategy is of course different, considering the mode and the season (winter or summer). As we work with data from March, we are in winter, so we will explain only the winter control rules.

Those rules are quite simple, as shown in *Figure 25*. The heat input is determined by the return air temperature T_{rair} and the supply air temperature T_{sair} . When we do not need at all to bring heat to building, the three systems are off:

- The heat recovery wheel does not turn
- The water do not circulate in the heating/cooling coil
- The water circulate in a close loop in the heating coil (water from the district heating is not used)

When a need of heating appears, the wheel of the heat recovery system starts to turn. With the increase of heat requirement the wheel turn faster until its maximal speed (as explained in "*System presentation - Rotary Heat Recovery System*" this maximal speed is reached when the efficiency of the heat recovery do not progress anymore). Then, if the heat requirement continues to increase, the water (provided by the heat pump) starts to circulate in the heating/cooling coil (valve opening) until the maximal flow rate. And finally if we still need more heat, the proportion of water provided by the district heating increases in the water heating coil flow rate (valve opening) until it will be only composed by district heating water. To resume, priority are:

- 1- Heat recovery System, LX01
- 2- Heating/cooling coil, LK40
- 3- Heating coil, LV40

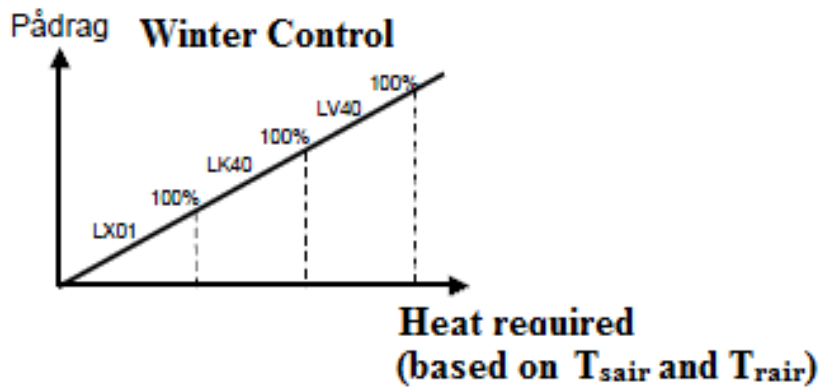


Figure 25. Winter control rules

Considering the fact that we have problems with valves position signals, the control rules that will appear with our measured data is probably not what it is supposed to be. In order to check that, we draw valves signals and heat recovery signal, in function of $T_{sair_des} - T_{sair}$ Figure 26.

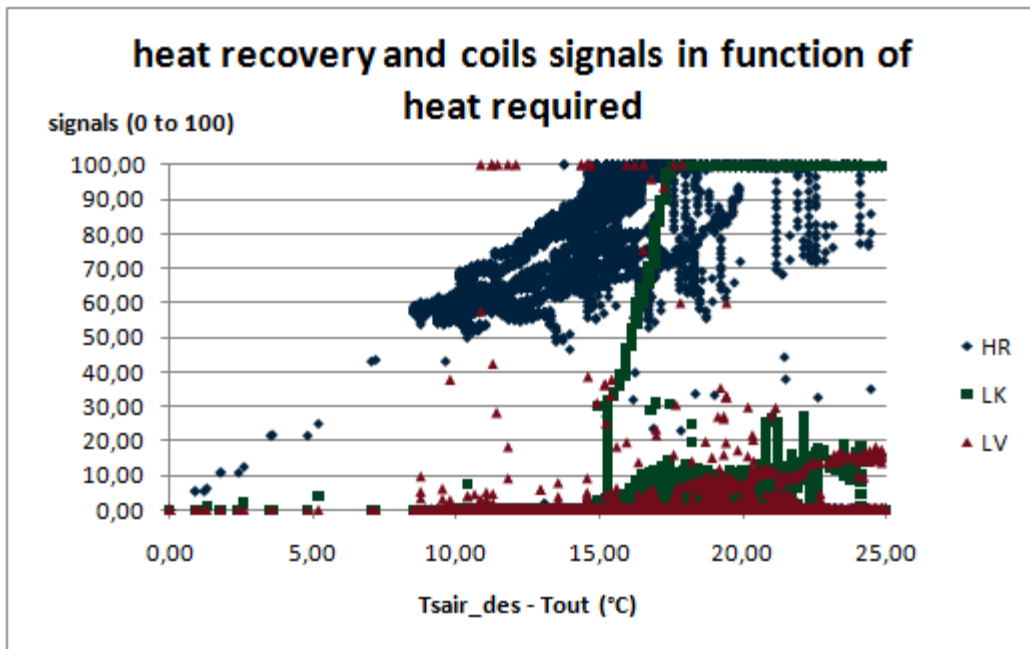


Figure 26. Control rules verification

The results in Figure 25 should be the similar to Figure 26, but as we expected results obtained do not correspond to the supposed rules, even if we can guess the rules application. Indeed, whereas we can see the increasing of the heat recovery and the heating/cooling coil signals, there are a lot of outliers for the both coils.

Energy Costs and CO₂ emission

Now we are going to calculate the energy costs and CO₂ emission induced by the results we got for the heat used and its distribution between the different components (heat recovery, heating/cooling coil, heating coil).

There are two primary consumptions sources for the heat production in our system:

- Electricity for the heating recovery (motor that make the wheel turn) and for the heating/cooling coil (compressor of the heat pump). The electricity for fans will not be considered.

- District heating (the heat of the district heating is produced by burning city wastes in Trondheim, but in other case it can be produced by burning other materials like wood, oil, gas, ..).

The electricity and district heating price is 1 NOK/kWh the and weight of CO₂ emission induced is 22 010 kg/kWh for the electricity if it is provided by hydro power (99%) and electricity mix UCPTÉ (1%) (see appendix: Primary energy factors and CO₂ emission coefficients) and 108 kg/kWh for the district heating if it is provided by burning city wastes, [14]. For each component we have to define the ratio between heat in kWh used and electricity (or district heating) in kWh in inlet. Then these ratios can be link to the electricity and district heating price and the weight of CO₂ emission. Thus we determine the ratios heat in kilowatt-hour produced/energy cost and heat in kilowatt-hour produced/ weight of CO₂ produced in kg

Rotary heat recovery system

The electricity used by the motor to turn the wheel is very low compare to heat recovered. Also when the wheel is turning we will consider that the motor use its maximal power 100 W to simplify the problem. Like we have a base time of data recording of one minute, if the wheel is turning, the electricity used will be 1.67 Wh/min. As a consequence the cost will be 1.67 Wh/min multiply by 1 NOK/kWh = 0.00167 NOK/min and the CO₂ emission will be 1.67 Wh/min multiply by 22 010 kg/kWh = 36.76 kg of CO₂/min.

Heating/cooling coil

This coil obtains heat from the heat pump as explained in *System Presentation – Air Handling Unit - Heating/Cooling Coil*. Also we can directly link the heat provided to the electricity used by using the heat pump COP in each recorded minute. We determine COP with *Equation 10*. We obtain the results shown in *Figure 27*:

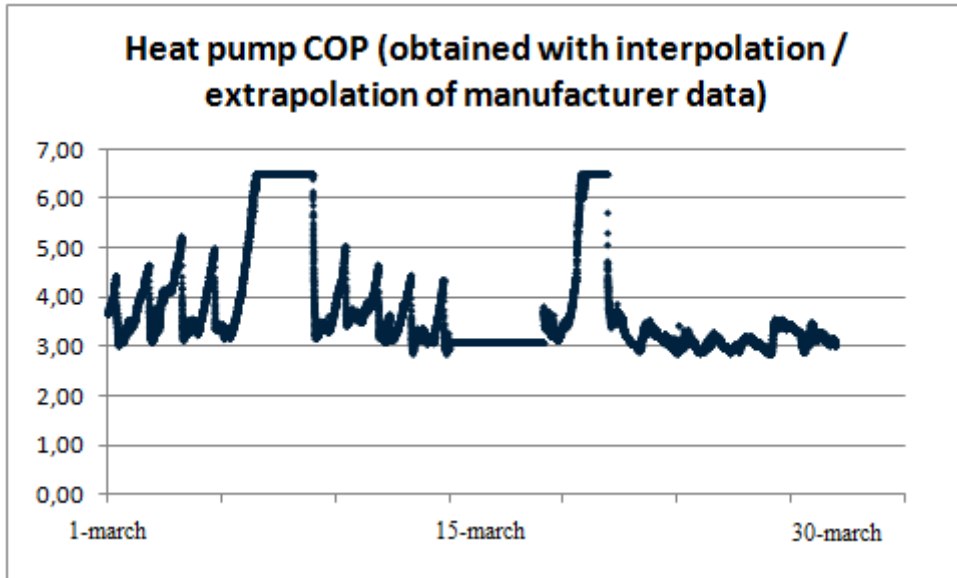


Figure 27. Heat pump COP (march 2011)

The cost and the weight in CO₂ emission will be:

$$Cost_{LK} = \frac{\dot{Q}_{LK_NTU}}{COP} \cdot el_price \quad (44)$$

$$CO2_{LK} = \frac{\dot{Q}_{LK_NTU}}{COP} \cdot el_CO2 \quad (45)$$

Heating coil

Like we neglect the pipe loss, the heat exchanged in this coil is directly equal to providing heat. Thus:

$$Cost_{LV} = \dot{Q}_{LV_NTU} \cdot dh_price \quad (46)$$

$$CO2_{LV} = \dot{Q}_{LV_NTU} \cdot dh_CO2 \quad (47)$$

With *el_price* and *dh_price* (electricity and district heating price), *el_CO₂* and *dh_CO₂* (electricity and district heating CO₂ emission).

Improved Control Strategies

The control strategies proposed are based on the costs or on the CO₂ emissions induced by the repartition of the heat exchanged between the three components.

If we want to optimize the cost, we will define for each minute the order of the most economic component to the most expensive (kWh of heat produce/NOK). In fact, just the COP variation can change this order and in every case the heat recovery system will be the most economical. The second most economical will be the heating/cooling coil If the

electricity price divided by the heat pump COP is inferior to the district heating price: $el_price/COP < dh_price$.

If we want to optimize the CO₂ emission, we will this time order the components from the least polluting to the the most polluting. Nevertheless, to do not totally ignore costs consideration, we will always use first the heat recovery system. We obtain the following winter control, presented in *Figure 28* for the cost strategy and in *Figure 29* for the CO₂ strategy.

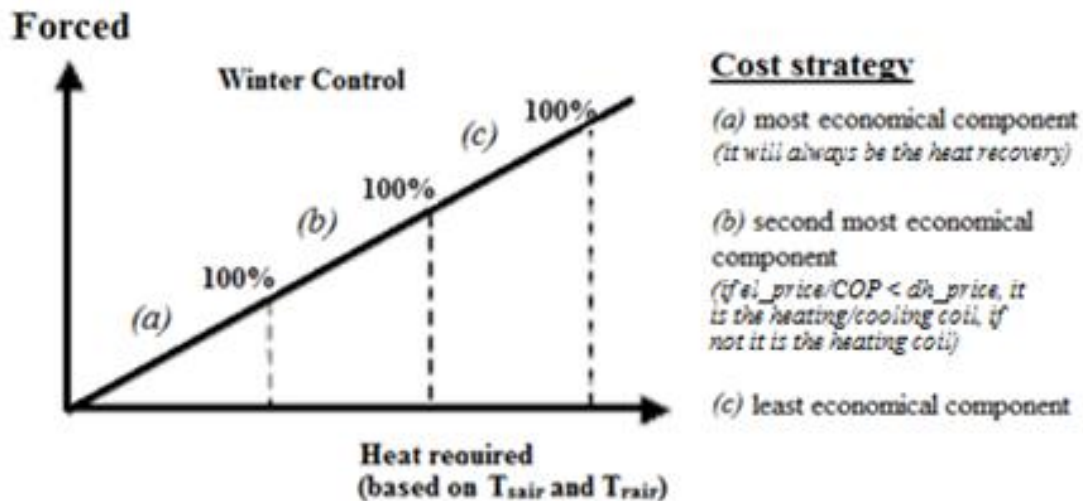


Figure 28. Improved control rules proposition: Cost strategy

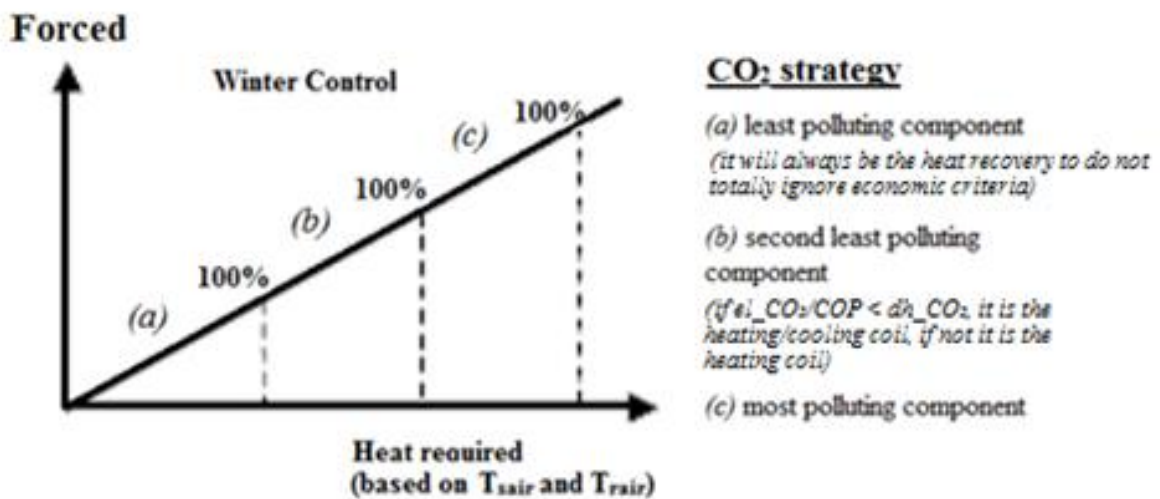


Figure 29. Improved control rules proposition: CO₂ strategy

We have to define to what power refers 100% of use for each component.

Regarding the coils we considered the manufacturer data, but we could have recalculated the maximal power for each minute with the NTU method (see *Combination of the NTU and valve position methods*).

For the heat recovery, we have in a first time to determine its maximal efficiency η_{hr_max} (efficiency with a signal equal to 100). It supposed to be around 0.8 ~ 0.9 considering rotary heat recovery theory. We obtain this characteristic (*Figure 30*):

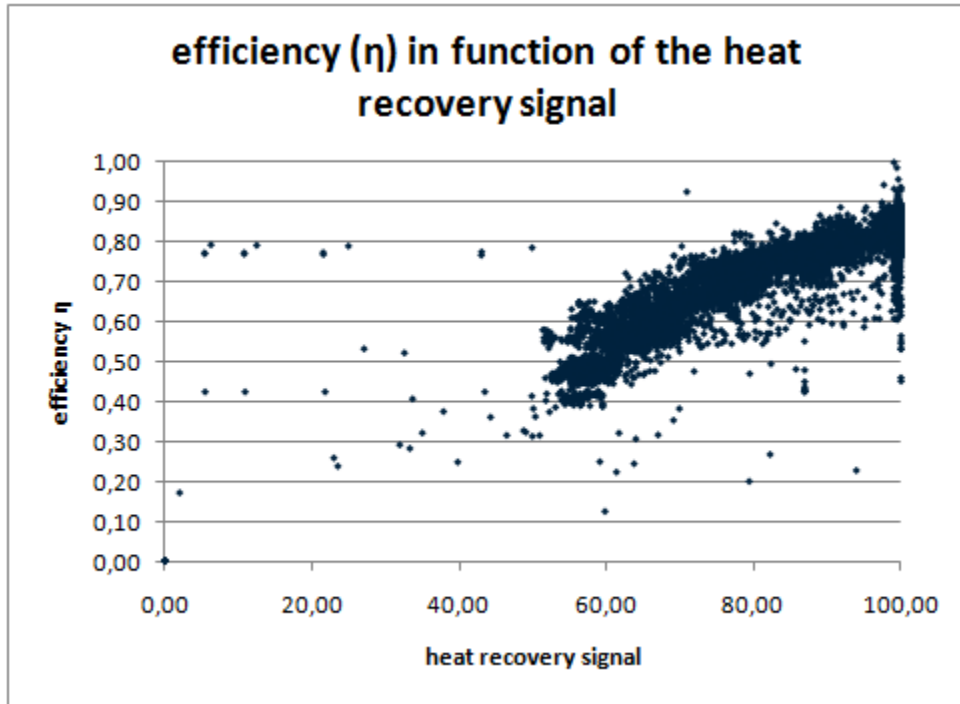


Figure 30. efficiency of the heat recovery in function of its measured signal

Thus, η_{hr_max} is equal to 0.85. As we know the return air temperature T_{rair} and the outside air temperature T_{out} , with the relation below (*Equation 48*), we can calculate the supply air temperature after heat recovery if the efficiency is maximal.

$$\eta = \frac{T_{sair_hr} - T_{sair}}{T_{rair} - T_{sair}} \quad (48)$$

Then we calculate the heat exchange in the heat recovery with this new T_{sair_hr} and the *Equation 18*. It will correspond to the maximal heating power of the heat recovery.

Current and proposed rules comparisons

Now we are going to study the difference in results obtained with the current and proposed rules. For that we will play with two things: First the ratio between district heating and electricity price; then the impact of the electricity and district heating sources. We will see how it affect the current and the propose rules results.

Regarding the electricity and district heating sources we consider the Trondheim case (electricity: hydro power (99%) + mix UCPT (1%), district heating: waste). With several ratio of district heating/electricity price, we obtained the results shown in *Figure 31*:

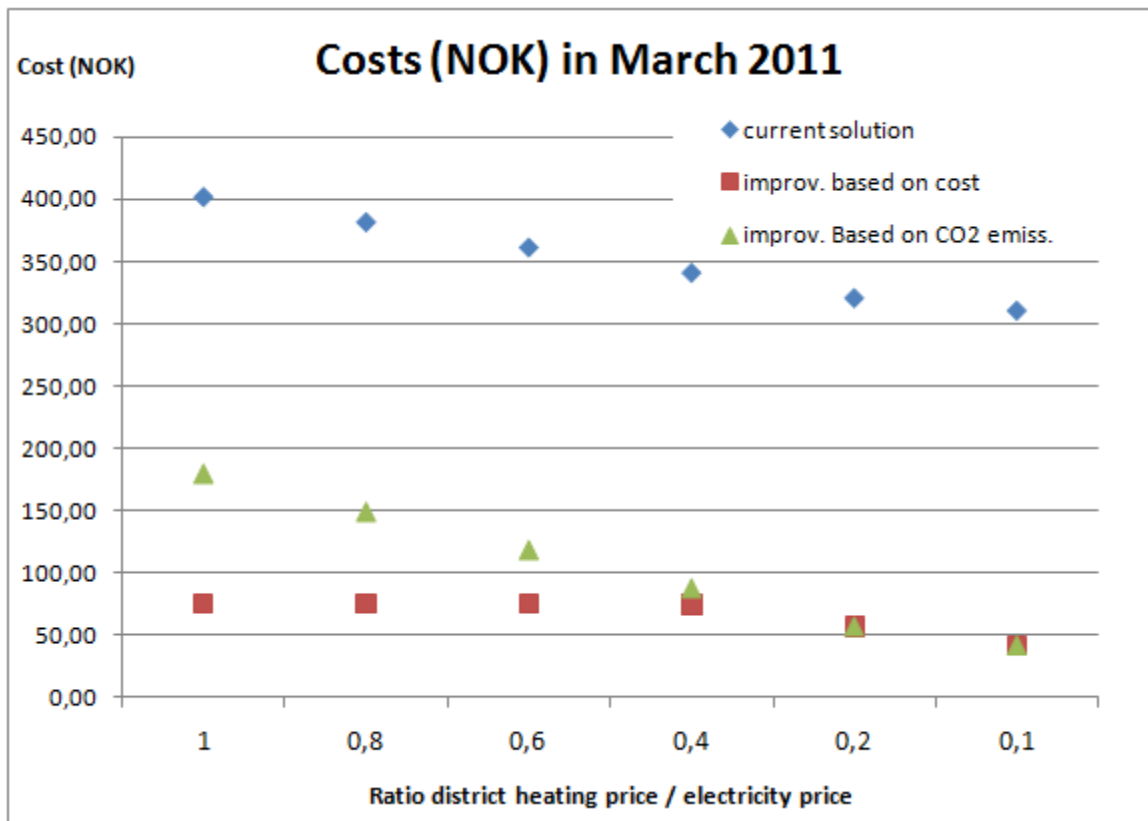


Figure 31. Impact of the ratio district heating/electricity price on the costs

In each case our improved solutions give better results than the current solution and so far. In fact, whereas the heat recovery is supposed to be the first element put in and the coils are supposed to be used when the heat recovery gives its maximal power, in reality it is not the case. Also our improvements are in majority due to the real application of this rule.

As we just decrease the price of the district heating in order to change the price ratio (district heating/electricity), the current solution cost is following this decrease.

With this configuration (electricity: hydro power (99%) + mix UCPT (1%), district heating: waste) and a price of one NOK/kWh for the district heating and the electricity, the heating/cooling coil is more interesting for the cost solution and the heating coil is more interesting for the CO₂ solution. However with the decreasing of the ratio, the use of the heating/cooling coil is less and less interesting for the cost solution, with no change for the heating coil regarding the CO₂ solution. So finally the heating coil becomes the most interesting for the both strategies (same results for the both solution with a price ratio of 0.1).

Regarding the electricity and district heating prices we consider what is approximately applied in Trondheim (1 NOK/kWh for the both). We test several combinations of electricity and district heating sources. We obtained the results shown in *Figure 32*:

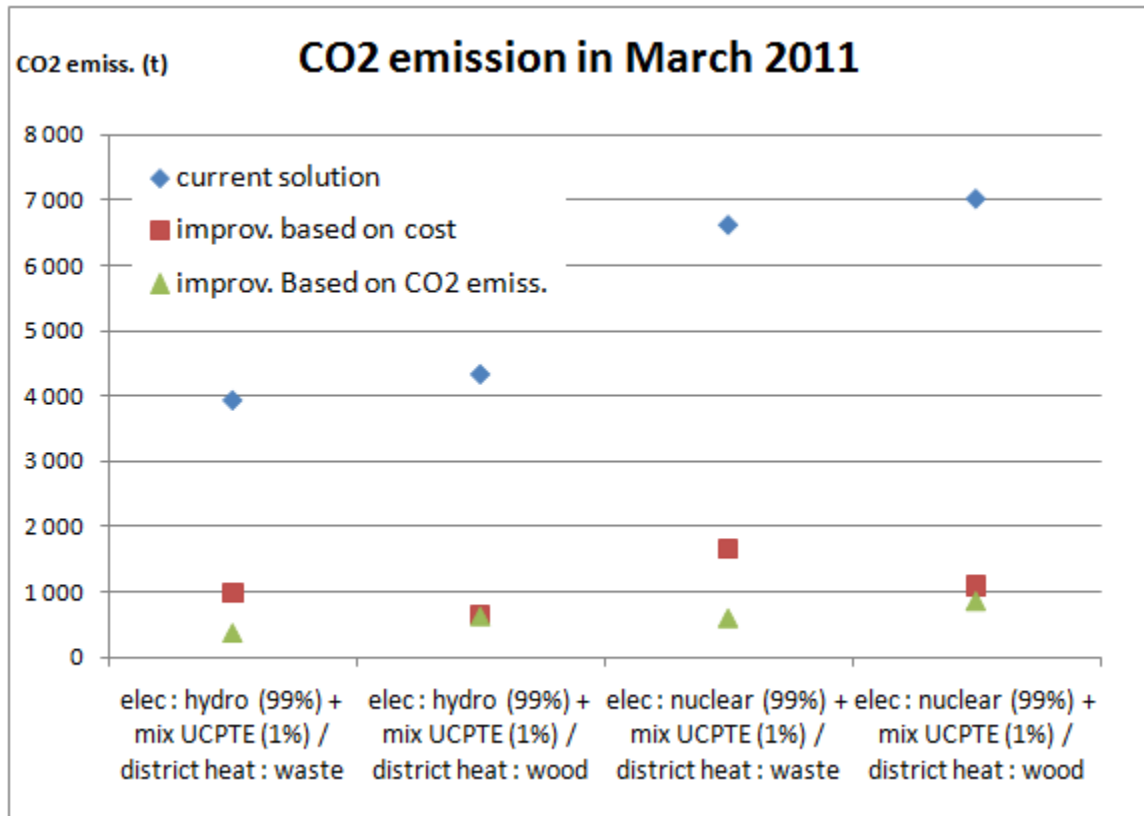


Figure 32. CO₂ emission regarding sources of electricity and district heating

As for the cost, our improvements give better results than the current solution. The same remark about the heat recovery can be made: the heat recovery is supposed to be the first element put in place and the coils are supposed to be used when the heat recovery gives its maximal power and in reality it is not the case. Also our improvements are in majority due to the real application of this rule.

In every case, as expected the improvement based on CO₂ give better results. However for the second configuration tested (electricity: hydro power (99%) + mix UCPTTE (1%), district heating: wood), results of the both improvements are really close. It means that the best solution for the costs was also the best solution for the CO₂ emissions.

In this study we test separately costs and CO₂ emission regarding price ratio and sources of electricity and district heating, Nevertheless in a real case these considerations have to be treated together.

Our improved strategies seem better compared to the current solution. However we have to consider this fact carefully. Indeed the method used to determine heat exchanged in each component has not been validated properly because of poor quality of measurement. Also, measurement quality has to be improved in a first place and then our optimized control strategies could be truly tested.

Conclusion

In this study we present several methods to determine the heat exchanged in each component of an air handling unit: heat balance, valve position method, NTU method. However we highlight the fact that poor quality of measured data can be a real problem to apply and validate those methods. Moreover the comparison of the NTU method and the valve position methods enable the detection of errors with valves position signals. This issue has also been confirmed by the use of the PCA method. Nevertheless, in this case the addition of a temperature sensor would be a quicker way to highlight this kind of problem.

In a second time new control strategies ventilation system, between heat recovery and two coils were analyzed in order to decrease energy cost and CO₂ emission. The purpose was to use firstly the cheaper or the most environmental friendly component. Those improvements were based on electricity and district heating cost and CO₂ emission. We show that in every case these two new improved strategies are better than the current strategy. Besides, regarding CO₂ emission, hydro power and heat based on waste as electricity and district heating sources offer one of the best solutions.

In reason of poor quality signals, it has been difficult to validate doubtlessly the heat exchanged calculations methods proposed. Considering optimization of the control strategy, the next step should be to define a multi-criteria optimized control strategy, which includes the criteria of the two improvements proposed: decrease of energy costs and CO₂ emission.

Acknowledgments

First of all, I wish to thank Natasa Djuric for her help, her patience, and her guidance throughout this all past year, during my project thesis and my master thesis.

I also thank Vojislav Novakovic, for permitting me and trusting me to accomplish my project thesis in the context of my Erasmus semester and for allowing me to continue my work in master thesis

And of course I would like to thank every people who allowed me to spend this year in Norway and consequently to do this master thesis, people from my home school (Grenoble Institute of Technology) and people from my host school (Norwegian University of Science and technology).

Appendix

Primary energy factors and CO₂ emission coefficients

	Primary energy factors f_p		CO ₂ production coefficient K
	Non-renewable	Total	kg/MWh
Fuel oil	1,35	1,35	330
Gas	1,36	1,36	277
Anthracite	1,19	1,19	394
Lignite	1,40	1,40	433
Coke	1,53	1,53	467
Wood shavings	0,06	1,06	4
Log	0,09	1,09	14
Beech log	0,07	1,07	13
Fir log	0,10	1,10	20
Electricity from hydraulic power plant	0,50	1,50	7
Electricity from nuclear power plant	2,80	2,80	16
Electricity from coal power plant	4,05	4,05	1340
Electricity Mix UCPTÉ	3,14	3,31	617

Source: Oekoinventare für Energiesysteme - ETH Zürich (1996).

These factors include the energy to build the transformation and transportation systems for the transformation of the primary energy to delivered energy.

References

- [1] European Environment Agency, EN16 Final Energy Consumption by Sector, Fig. 4: Final energy consumption (million TOE) and per capita final consumption, EU-27; (2008)
- [2] N. Djuric, V. Novakovic, Correlation between standards and the lifetime commissioning; Energy Buildings (2009); DOI:10.1016/j.enbuild.2009.10.020.
- [3] Shengwei Wang, Fu Xiao, AHU sensor fault diagnosis using principal component analysis method; energy and buildings 36 (2004) 147-160; DOI:10.1016/j.enbuild.2003.10.002
- [4] Qiang Zhou, Shengwei Wang, Zhenjun Ma, A model-based fault detection and diagnosis strategy for HVAC systems ; Int. J. Energy Res. 2009; 33:903–918; DOI: 10.1002/er
- [5] Shengwei Wang, Qiang Zhou, Fu Xiao; A system-level fault detection and diagnosis strategy for HVAC systems involving sensors faults; Energy and buildings 42 (2010) 477-490; DOI: 10.1016/j.enbuild.2009.10.017
- [6] F. Leboeuf; project thesis: Advanced analysis of measured data for efficient operation of modern buildings
- [7] Air cooled water chiller, engineering manual EDM AQT-A.1GB, September 2008
- [8] N. Djuric, et al., Data fusion heat pump performance estimation, Energy Buildings (2010); DOI:10.1016/j.enbuild.2010.11.003
- [9] ASHRAE Systems and Equipment Handbook 2000
- [10] Systemair specifications
- [11] J.E. Jackson, A Users Guide to Principal Components, Wiley & Sons Inc., New York, 1991.
- [12] The Unscrambler (software), PCA method reference, Introduction to Principal Component Analysis (PCA)
- [13] The Unscrambler (software), Interpreting PCA plots
- [14] A.W. Larsen, T. Astrup, CO2 emission factors for waste incineration: Influence from source separation of recyclable materials, 2011 *Waste Management* 31 (7), pp. 1597-1605 0